

Legends for Supplemental Figures

Fig. S1. Detailed study overview. (A) PRS-PheWAS and PRS-LabWAS analyses using the external European-ancestry IAMDGC GWAS of AMD (8) as a base for scoring subjects in MVP. (B) Ancestry-specific GWAS analyses, and multi-ancestry meta-analysis, with corresponding secondary analyses including TWAS and Mendelian randomization (EA-only), and fine-mapping (EA and trans-ancestry). An unrelated MVP EA tranche was used as a replication cohort, and meta-analyzed into final EA and multi-ancestry meta-analyses. (C) HLA fine-mapping and rare variant analysis.

Fig. S2. PRS distribution of AMD cases and controls. (A) EA samples in MVP; (B) AA samples in MVP; and (C) HA samples in MVP. The PRS was constructed using weights derived from the IAMDGC GWAS (8).

Fig. S3. Regional association plots of novel loci from the European-ancestry replication meta-analysis (57,290 cases, 324,430 controls). The 1000 Genomes EUR panel was used as the reference for plotting LD r^2 .

Fig. S4. QQ plots of the multi-ancestry GWAS and meta-analysis. (A) MVP AA GWAS, (B) MVP HA GWAS, (C) EA meta-analysis, and (D) multi-ancestry meta-analysis. SNPs with minor allele frequency greater than 0.5% are plotted and included in the genomic control inflation calculation.

Fig. S5. Conditional analysis of *PLTP* and *MMP9* signals in the 20q13 locus. Regional association plots of: (A) the EA replication meta-analysis, demonstrating a primary signal near *PLTP*; (B) the IAMDGC study (8), demonstrating a primary signal near *MMP9*; (C) the EA meta-analysis conditioned on the index SNP from the IAMDGC study (rs1888235); (D) the IAMDGC study conditioned on the index SNP from the EA meta-analysis (rs17447545). LD r^2 values were calculated in the MVP EA cohort. The dashed line denotes genome-wide significance (5×10^{-8}).

Fig. S6. Genome-wide significant loci from the AA and HA GWAS in MVP. (A) Regional association plot of the *HLA-DQB1* locus from the AA GWAS (2,302 cases, 29,223 controls). The 1000 Genomes AFR panel was used as the reference for plotting LD r^2 . (B-C) Regional association plots of the *CFH* and *ARMS2-HTRA1* loci from the HA GWAS (1,656 cases, 10,819 controls). The 1000 Genomes AMR panel was used as the reference for plotting LD r^2 .

Fig. S7. Novel genome-wide significant loci from the multi-ancestry meta-analysis. Regional association plots of novel loci from the multi-ancestry replication meta-analysis (61,258

cases, 364,472 controls) beyond that reported for the EA meta-analysis. The 1000 Genomes EUR panel was used as the reference for plotting LD r^2 .

Fig. S8. Co-localization of GWAS and eQTL signals identifies candidate causal variants. Shown are significant co-localized signals (co-localization posterior probability > 0.01) from the multi-ancestry discovery meta-analysis using the mmQTL (31) method.

Fig. S9. Characterization of TWAS results across tissues. **(A)** Pearson correlation of AMD association z-scores across the 38 tissues analyzed from GTEx, EyeGEx, STARNET, and PEC. **(B)** Hierarchical clustering of tissues based on AMD associations using Ward's linkage method.

Fig. S10. Regional Miami plots of genes with novel TWAS associations. The TWAS was based on the DLPFC brain model jointly testing genes and transcript isoforms. Results are based on the EA discovery meta-analysis (45,045 cases, 275,806 controls). The GWAS p-values are shown above the $y=0$ line, and the TWAS p-values are shown below it. SNPs are colored according to linkage disequilibrium r-squared with the lead SNP (EA panel). Lines connecting SNP predictors of genetically regulated gene expression are colored according to the significance level of the SNP: orange, $p \leq 5 \times 10^{-8}$; cyan, $p \leq 1 \times 10^{-5}$; gray, $p > 1 \times 10^{-5}$.

Fig. S11. Gene set enrichment analysis (GSEA) of TWAS genes. **(A)** GSEA of TWAS using the DLPFC transcripts (genes and isoforms) model, and **(B)** the multi-tissue meta-analysis. Shown are the top ten enrichments by effect size (odds ratio) in both analyses.

Fig. S12. Semantic clustering of enriched gene ontology (GO) terms in the AMD multi-tissue transcriptome-wide association study (TWAS) identifies immune and lipid homeostasis functions. First, we performed enrichment of AMD TWAS associated genes (FDR < 0.05 in ACAT meta-analysis of all tissues) for GO terms corresponding to ontologies of molecular functions (MFO), biological processes (BPO), and cellular components (CCO). Semantic clustering of the GO terms that had enrichment FDR < 0.1 (Fisher's exact test) and could be clustered identified 7 clusters (BPO1-BPO5, CCO1, and MFO1). For each of these clusters we provide a word cloud based on the description of the GO terms where words that appear more frequently are larger; clusters are ordered from left to right and top to bottom from the most significant to the least significant based on their meta-analyzed p-value (ACAT). Major themes that are associated with AMD are immune functions and lipid homeostasis.

Fig. S13. Enrichment of rare variant burden associations in TWAS meta-analysis genes. TWAS meta-analysis genes were those with FDR < 0.05; only protein-coding genes were considered. *** FDR < 0.001, ** FDR < 0.01, * FDR < 0.05 (12 rare variant gene sets were

considered from the rare variant analysis). Mask 1: Loss of function mutations only; Mask 2: Loss of function + missense mutations; Mask 3: Loss of function + missense + splice mutations.

Captions for Supplemental Tables

Table S1. Sample demographics for the GWAS cohorts comprising the European-ancestry meta-analysis and multi-ancestry meta-analysis.

Table S2. (A) Effects of demographic parameters on AMD case/control status in the MVP EA, AA and HA samples, estimated in single regression models. (B) Effects of demographic parameters on AMD case/control status in the MVP EA, AA and HA samples, estimated in multiple regression models. (C) Multi-ancestry time-to-AMD-diagnosis analysis using a Cox proportional-hazards model.

Table S3. PheWAS summary statistics of the IAMDGC-derived PRS in European-ancestry subjects in MVP. The PRS was normalized to the unit normal distribution.

Table S4. LabWAS summary statistics of the IAMDGC-derived PRS in European-ancestry subjects in MVP. The PRS was normalized to the unit normal distribution and labs were inverse rank normal transformed (IRNT).

Table S5. Index SNPs from genome-wide significant loci in the European-ancestry replication meta-analysis (N=57,290 cases, 324,430 controls).

Table S6. Comparison of effect sizes at the index SNPs across the IAMDGC, GERA, MVP Replication GWAS.

Table S7. Conditionally independent genome-wide significant markers from the European replication meta-analysis.

Table S8. Genetic correlation of AMD with selected eye-related traits.

Table S9. Genetic correlation of AMD with blood-based biomarkers, hematological parameters, and other traits. Trait GWAS were from the Pan-UKB project unless noted otherwise. Genetic correlation analysis was conducted separately in the EA meta-analysis and EA replication GWAS, and rG effect sizes were meta-analyzed using inverse variance-weighted fixed effects meta-analysis.

Table S10. Mendelian randomization analyses of pigmentation traits on AMD. Traits were tested using five methods implemented in the TwoSample MR package: Inverse variance weighted, MR Egger, simple mode, weighted mode, and weighted median. Horizontal pleiotropy was tested via the MR Egger intercept.

Table S11. Index SNPs from genome-wide significant loci in the African-ancestry GWAS (N=2,302 cases, 1,656 controls).

Table S12. LabWAS summary statistics of the MVP AA GWAS-derived PRS in unrelated African-ancestry subjects in MVP not used in the GWAS cohort. The PRS was normalized to the unit normal distribution and labs were inverse rank normal transformed (IRNT). A PheWAS was also performed, with no significant associations.

Table S13. Index SNPs from genome-wide significant loci in the Hispanic/Latino-ancestry GWAS (N=1,656 cases, 10,819 controls).

Table S14. Index SNPs from genome-wide significant loci in the multi-ancestry replication meta-analysis (N=61,248 cases, 364,472 controls).

Table S15. SNPs with posterior probability > 0.01 from fine-mapping the European-ancestry discovery meta-analysis (N=45,045 cases, 275,806 controls). Fine-mapping was conducted at each genome-wide significant locus using FINEMAP (30) software.

Table S16. SNPs with posterior probability > 0.01 from fine-mapping the multi-ancestry discovery meta-analysis (N=49,003 cases, 315,848 controls). Fine-mapping was conducted at each genome-wide significant locus using FINEMAP (30) software.

Table S17. Candidate causal variants from eQTL co-localization analysis using the mmQTL method (31). Shown are SNPs with co-localization posterior probability (CLPP) greater than 0.01. a) eQTL co-localization with the trans-ancestry fine-mapping. b) eQTL co-localization with the European-ancestry fine-mapping.

Table S18. Local ancestry analysis of haplotypes at *CFH* in admixed MVP populations. a) Enrichment of European-ancestry haplotypes (EUR) in AA AMD cases. b) Enrichment of individuals with homozygous European ancestry at *CFH* (EUR/EUR) in AA AMD cases. c) Enrichment of EUR haplotypes, compared to non-EUR haplotypes in HA AMD cases. d) Enrichment of EUR haplotypes in HA AMD cases, compared to African (AFR) and Native American (NAT) haplotypes.

Table S19. Haplotype analysis of the *CFH* locus in admixed African-ancestry (AA) subjects. Case and control frequencies were derived for all haplotypes and stratified by individuals with homozygous African local ancestry (AFR/AFR) or homozygous European local ancestry (EUR/EUR). a) Haplotype model used in Cipriani et al (38). b) Haplotype model used in Pappas et al (39).

Table S20. Local ancestry analysis of haplotypes at the ARMS2 locus in admixed MVP populations. **(A)** No significant enrichment of European-ancestry haplotypes (EUR) in AA AMD cases. **(B)** No significant enrichment of individuals with homozygous European ancestry at ARMS2 (EUR/EUR) in AA AMD cases. **(C)** No significant enrichment of EUR haplotypes, compared to non-EUR haplotypes in HA AMD cases. **(D)** Slight enrichment of Native American (NAT) haplotypes in HA AMD cases, compared to African (AFR) and EUR.

Table S21. Modeling epistatic interaction between the *CFH* Y402H and ARMS2 A69S risk alleles in MVP EA subjects. **(A)** Summary statistics of the model including the A69S*Y402H multiplicative interaction term. **(B)** Summary statistics of the model excluding the multiplicative interaction term. **(C)** Likelihood ratio test comparing the two models.

Table S22. HLA fine-mapping summary statistics for unrelated EA subjects in MVP. Association with AMD was tested for four-digit alleles at *HLA-A*, *B*, *C*, *DPB1*, *DQA1*, *DQB1*, and *DRB1* imputed by HIBAG software (41), considered additively with all other alleles as reference. Association was tested using two models: 1) sex and ten within-ancestry PCs only, and 2) sex, ten within-ancestry PCs, and risk allele dosages for *CFH* (rs1061170), ARMS2 (rs10490924), *CFB/C2* (rs429608), and *C3* (rs2230199). Firth logistic regression (80) was used for both models; p-values and confidence intervals are based on the penalized likelihood ratio test. Alleles with minor allele count less than 50 were excluded from analysis.

Table S23. HLA fine-mapping summary statistics for unrelated AA subjects in MVP. Association with AMD was tested for four-digit alleles at *HLA-A*, *B*, *C*, *DPB1*, *DQA1*, *DQB1*, and *DRB1* imputed by HIBAG software (41), considered additively with all other alleles as reference. Association was tested using two models: 1) sex and ten within-ancestry PCs only, and 2) sex, ten within-ancestry PCs, and risk allele dosages for *CFH* (rs1061170), ARMS2 (rs10490924), *CFB/C2* (rs429608), and *C3* (rs2230199). Firth logistic regression (80) was used for both models; p-values and confidence intervals are based on the penalized likelihood ratio test. Alleles with minor allele count less than 50 were excluded from analysis.

Table S24. HLA fine-mapping summary statistics for unrelated HA subjects in MVP. Association with AMD was tested for four-digit alleles at *HLA-A*, *B*, *C*, *DPB1*, *DQA1*, *DQB1*, and *DRB1* imputed by HIBAG software (41), considered additively with all other alleles as reference. Association was tested using two models: 1) sex and ten within-ancestry PCs only, and 2) sex, ten within-ancestry PCs, and risk allele dosages for *CFH* (rs1061170), ARMS2 (rs10490924), *CFB/C2* (rs429608), and *C3* (rs2230199). Firth logistic regression (80) was used for both models; p-values and

confidence intervals are based on the penalized likelihood ratio test. Alleles with minor allele count less than 50 were excluded from analysis.

Table S25. Transcriptome-wide association scan (TWAS) summary statistics using the brain DLPFC (PsychENCODE) tissue model (N=45,045 cases, 275,806 controls).

Table S26. Transcriptome-wide association scan (TWAS) summary statistics using the retina (EyeGEx) tissue model (N=45,045 cases, 275,806 controls).

Table S27. TWAS summary statistics from the ACAT meta-analysis of 37 tissue models (N=45,045 cases, 275,806 controls).

Table S28. Summary-based Mendelian randomization (SMR) summary statistics for retina gene expression instruments (EyeGEx) (N=45,045 cases, 275,806 controls).

Table S29. Gene-set enrichment analysis (GSEA) summary statistics based on the DLPFC TWAS.

Table S30. Gene-set enrichment analysis (GSEA) summary statistics based on the TWAS tissue meta-analysis.

Table S31. Summary statistics from the gene-based rare variant burden test. All SNPs were ultra-rare (frequency less than 0.25%) and genotyped on the MVP 1.0 array (72). Three masks were defined: mask1, containing only frameshift, nonsense, stop-gained, and stop-loss loss of function (LoF) SNPs; mask2 containing LoF SNPs plus high-impact missense variants; and mask3, containing LoF + missense + high-impact splice-site mutations. Burden tests over the masks were conducted in REGENIE (75).

Table S32. Comparison of the AMD TWAS results to previous studies (49, 70).

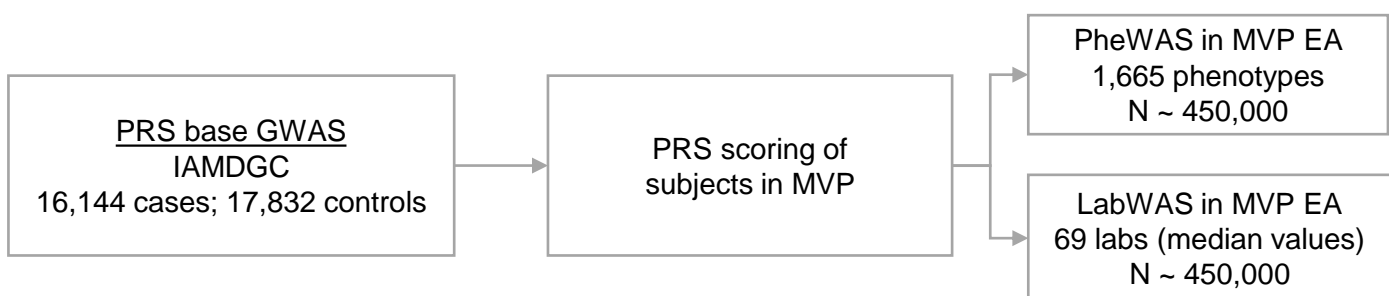
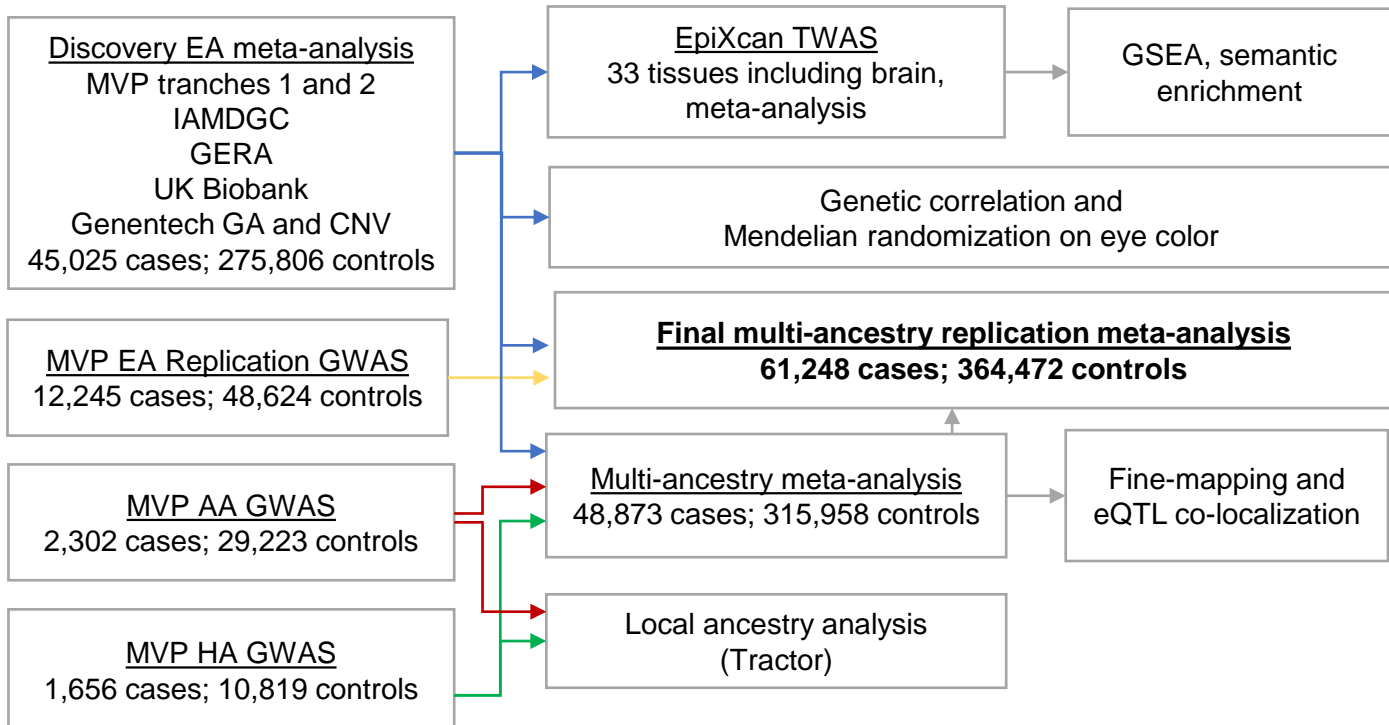
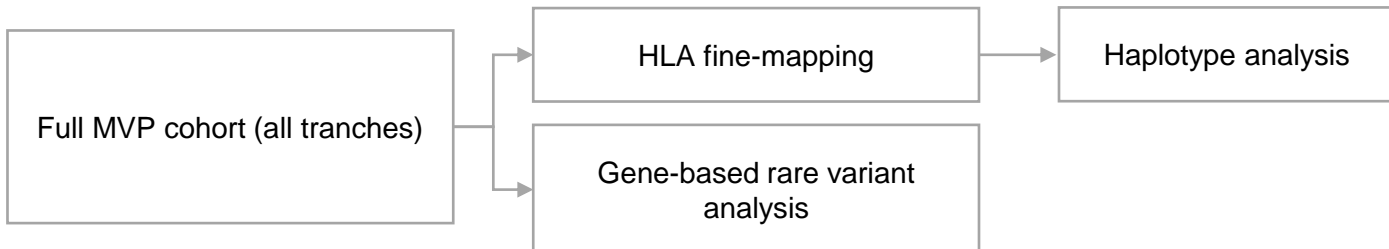
A**AMD IAMDGC-PRS PheWAS/LabWAS****B****GWAS and TWAS analyses****C****Rare variant analysis and HLA fine-mapping**

Fig. S1. Detailed study overview. (A) PRS-PheWAS and PRS-LabWAS analyses using the external European-ancestry IAMDGC GWAS of AMD (8) as a base for scoring subjects in MVP. (B) Ancestry-specific GWAS analyses, and multi-ancestry meta-analysis, with corresponding secondary analyses including TWAS and Mendelian randomization (EA-only), and fine-mapping (EA and trans-ancestry). An unrelated MVP EA tranche was used as a replication cohort, and meta-analyzed into final EA and multi-ancestry meta-analyses. (C) HLA fine-mapping and rare variant analysis.

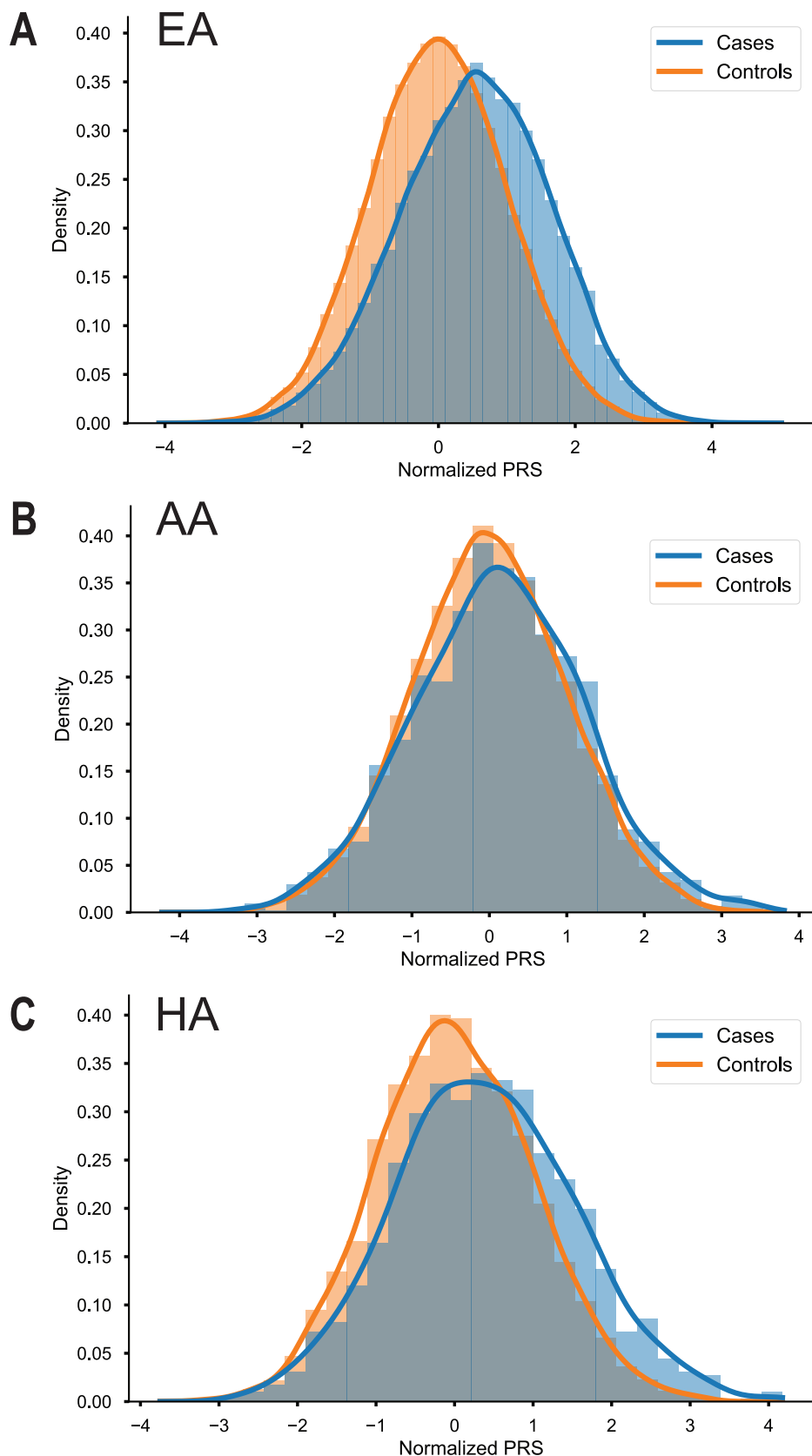
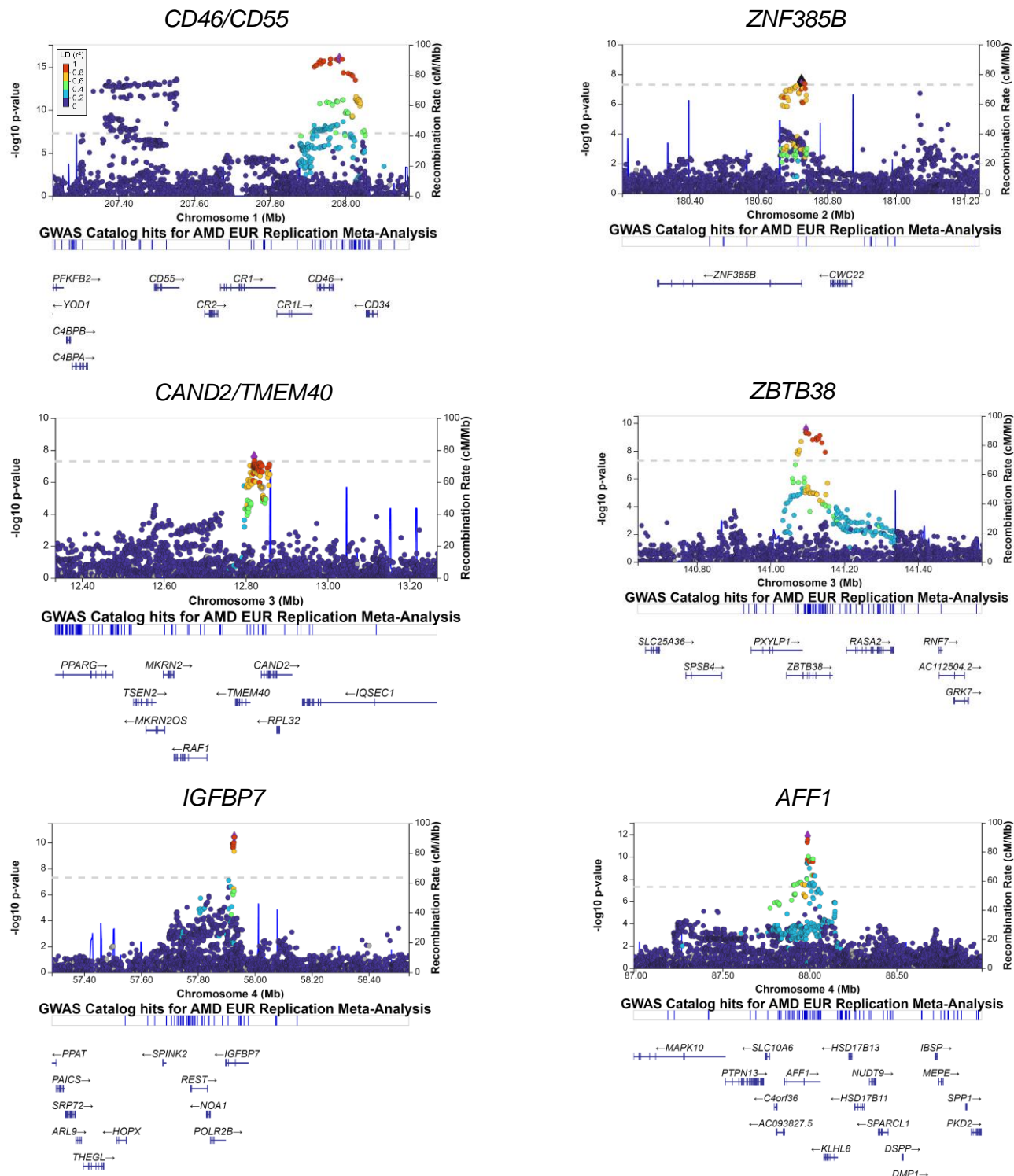
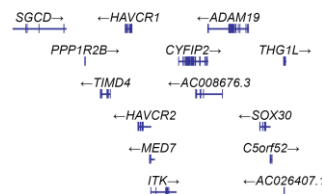
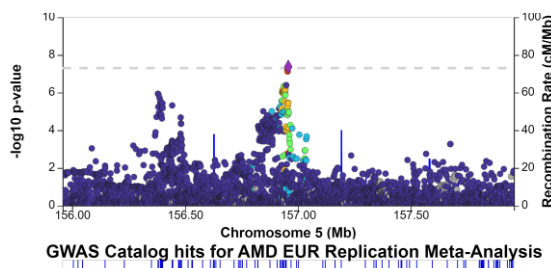


Fig. S2. PRS distribution of AMD cases and controls. (A) EA samples in MVP; (B) AA samples in MVP; and (C) HA samples in MVP. The PRS was constructed using weights derived from the IAMDGC GWAS (8).

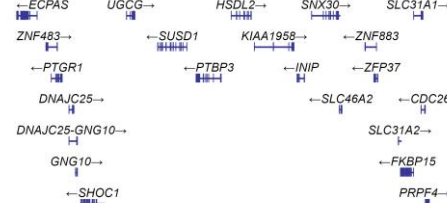
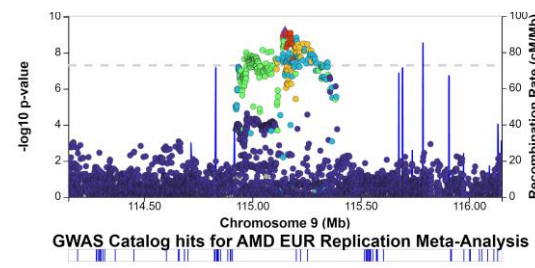
Fig. S3. Novel genome-wide significant loci from the European-ancestry meta-analysis. Regional association plots of novel loci from the European-ancestry replication meta-analysis (N=57,290 cases, 324,430 controls). The 1000 Genomes EUR panel was used as the reference for plotting LD r^2 .



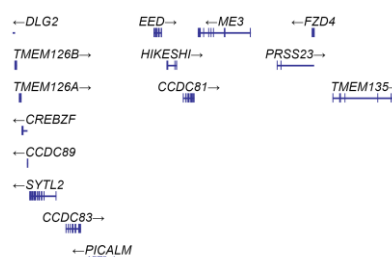
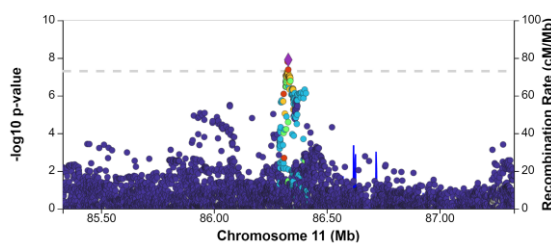
ADAM19



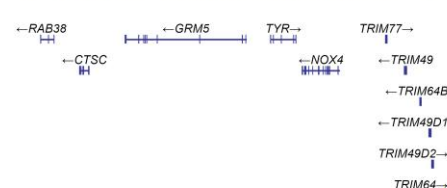
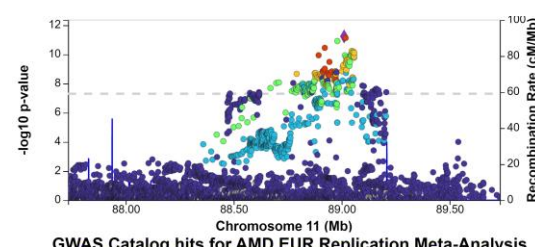
HSDL2



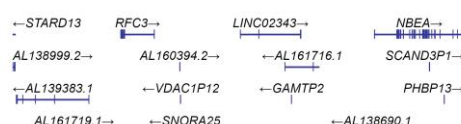
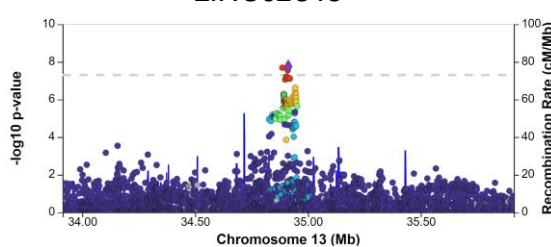
ME3



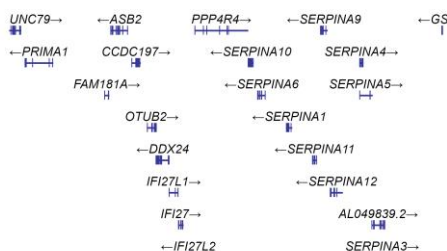
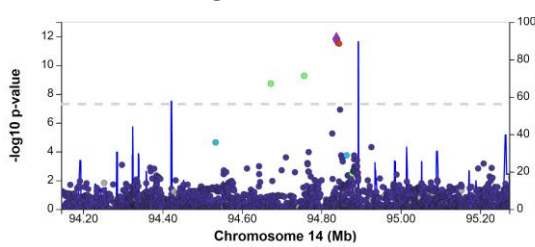
TYR



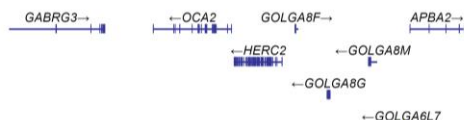
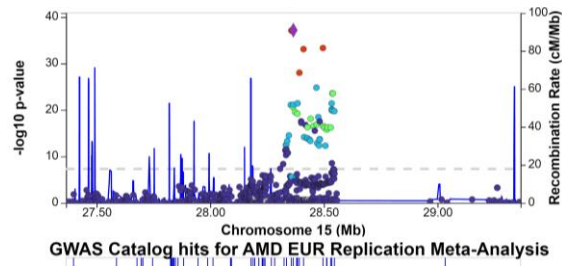
LINC02343



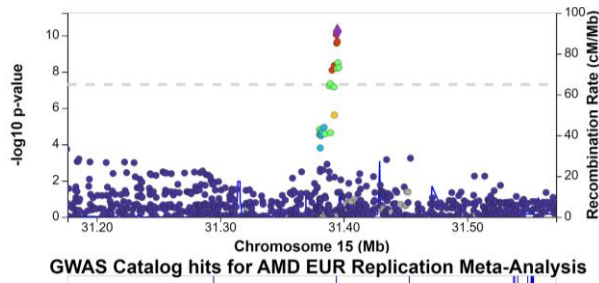
SERPINA1



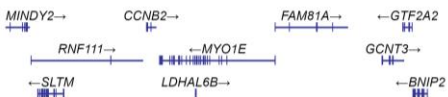
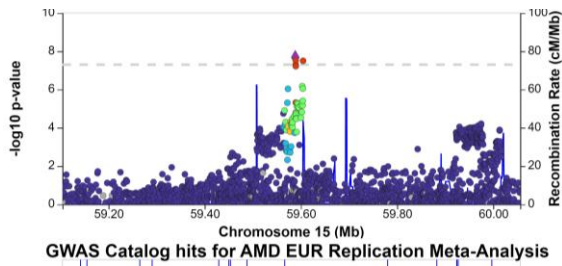
HERC2/OCA2



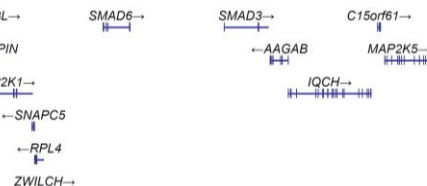
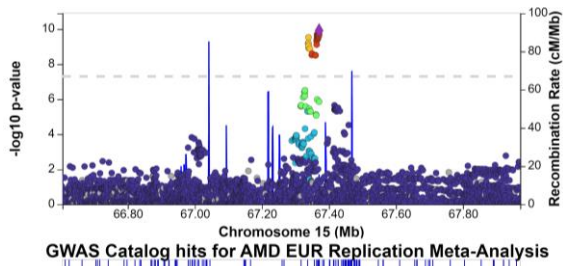
TRMP1



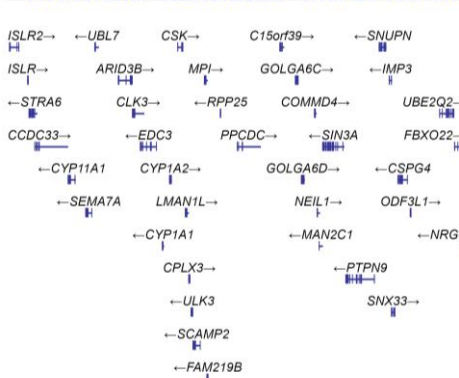
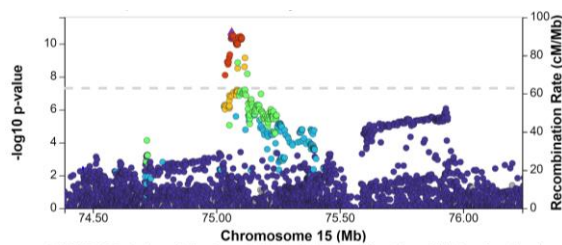
MYO1E



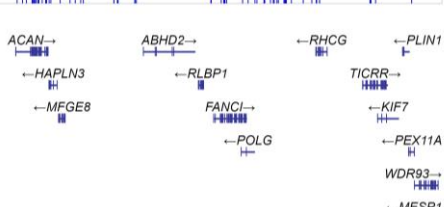
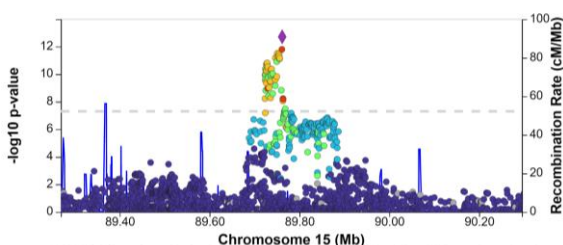
SMAD3



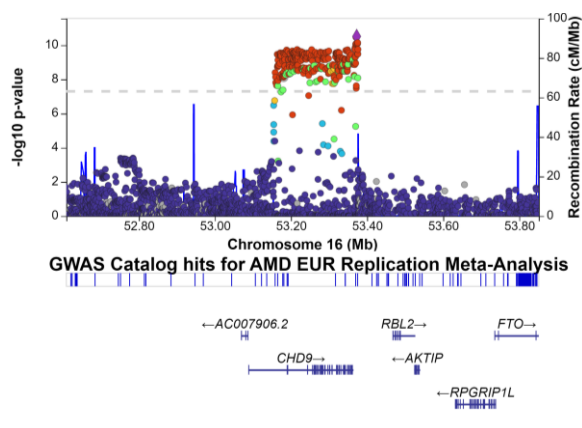
CSK



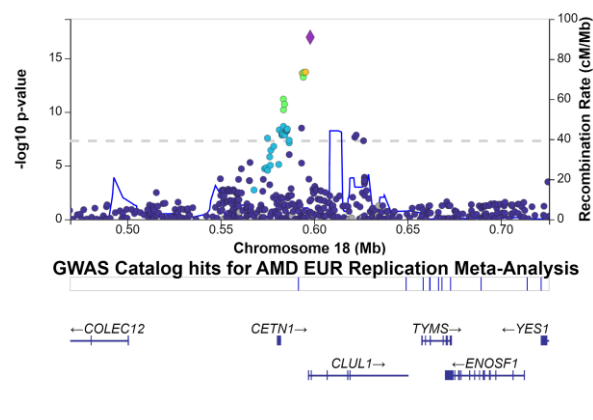
RLBP1



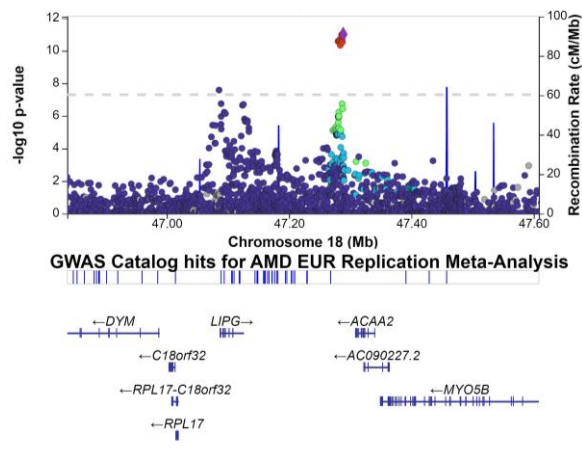
CHD9



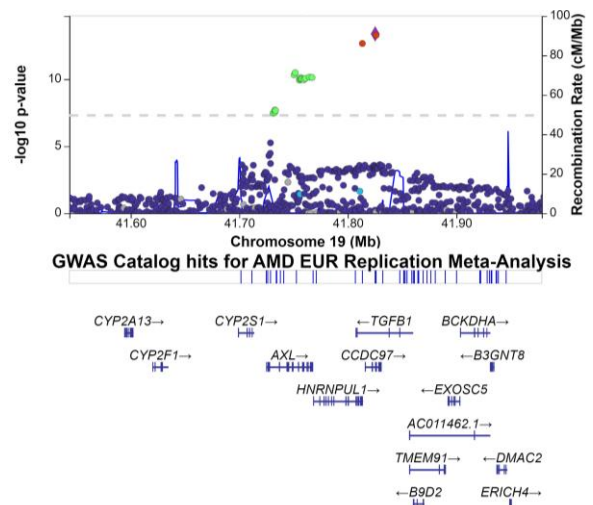
CLUL1



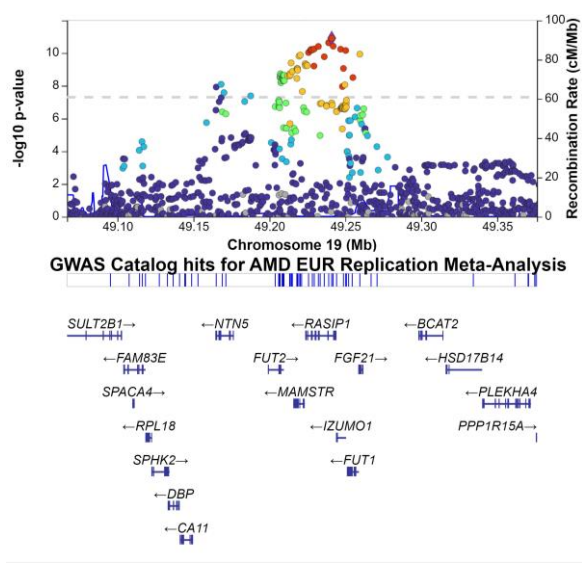
ACAA2/LIPG



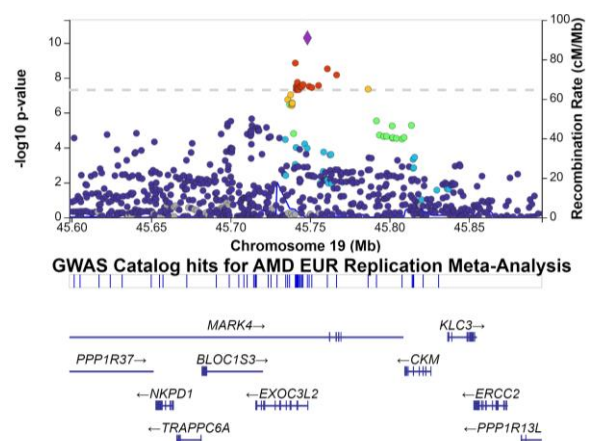
TGFB1



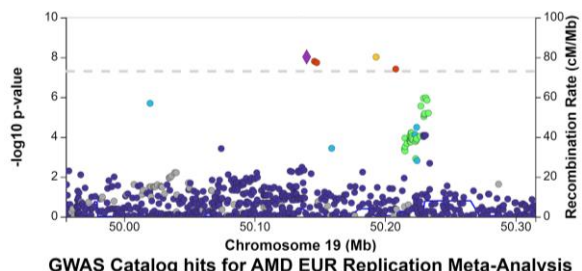
RASIP1



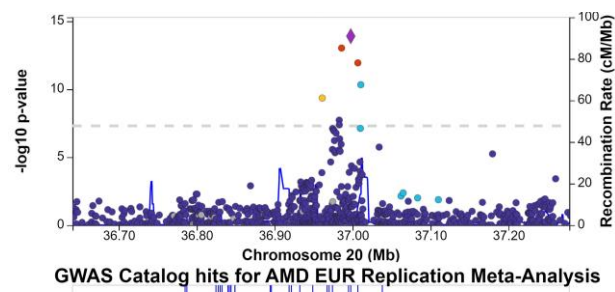
MARK4/EXOC3L2



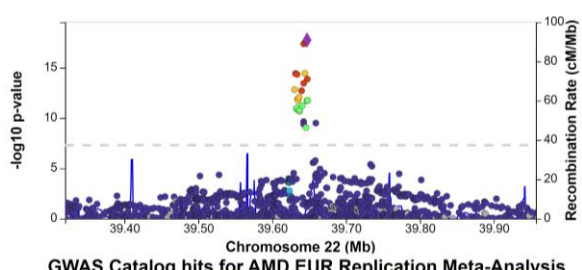
RRAS



LBP



PDGFB



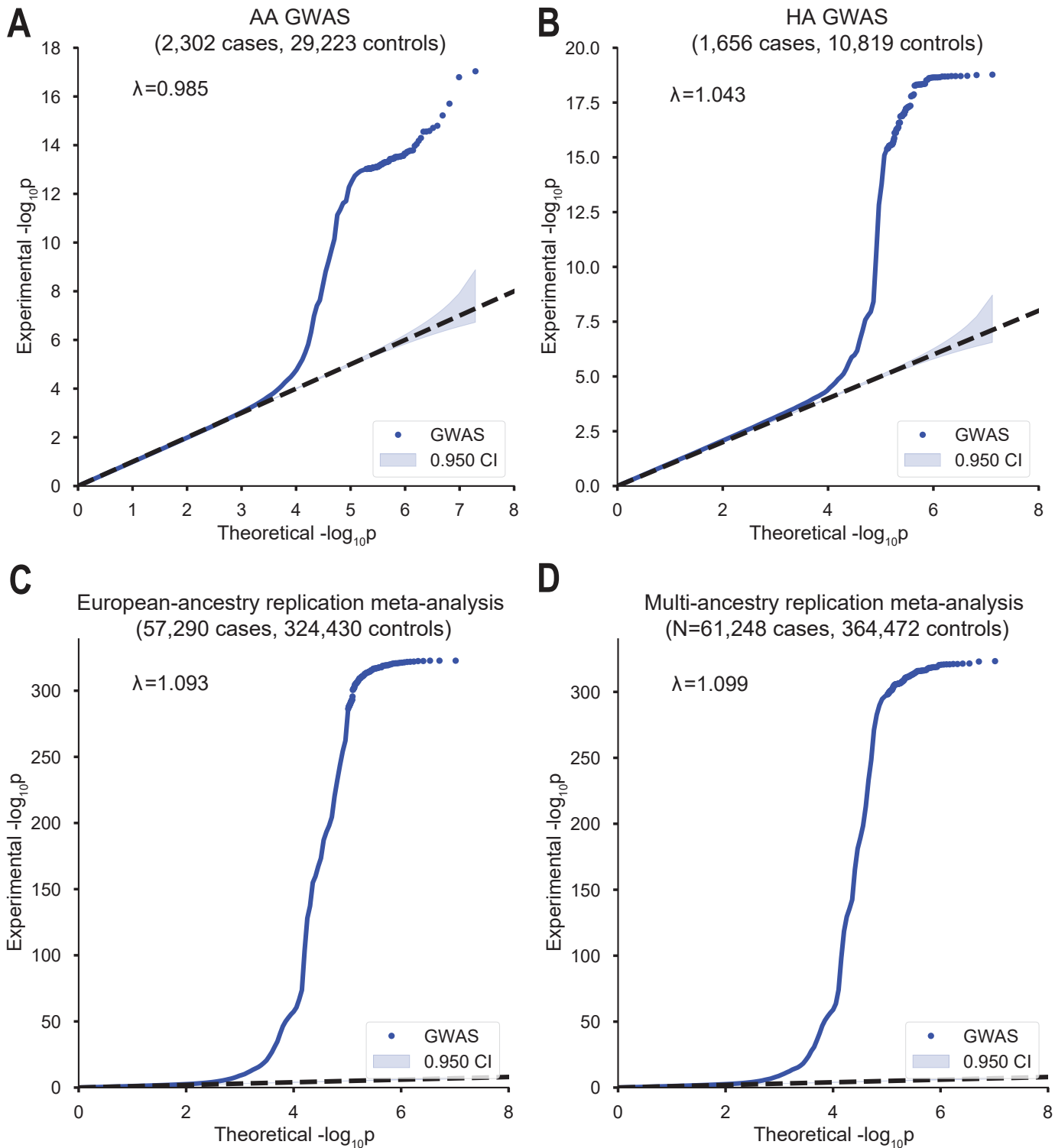


Fig. S4. QQ plots of the multi-ancestry GWAS and meta-analysis. (A) MVP AA GWAS, (B) MVP HA GWAS, (C) EA meta-analysis, and (D) multi-ancestry meta-analysis. SNPs with minor allele frequency greater than 0.5% are plotted and included in the genomic control inflation calculation.

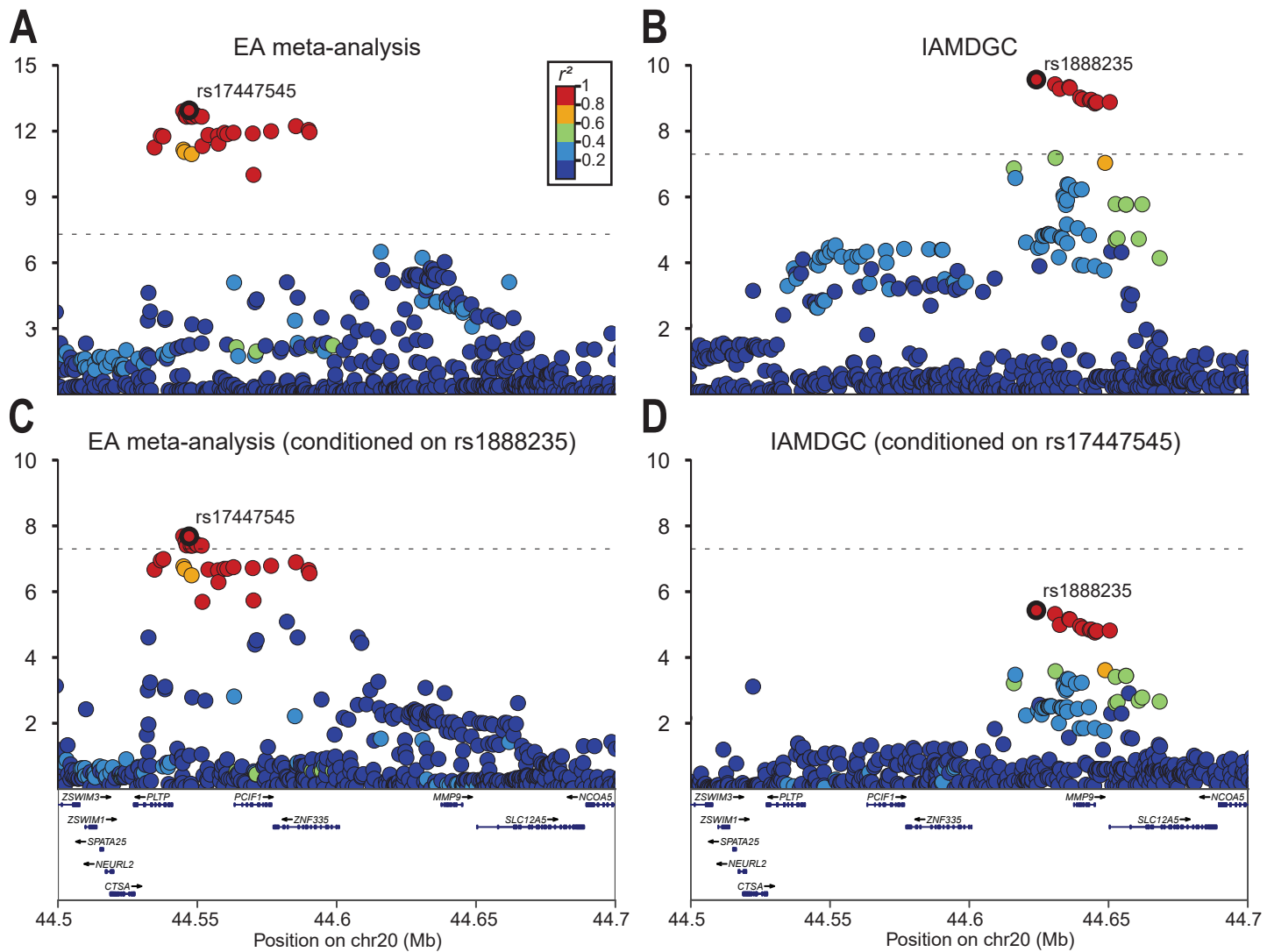
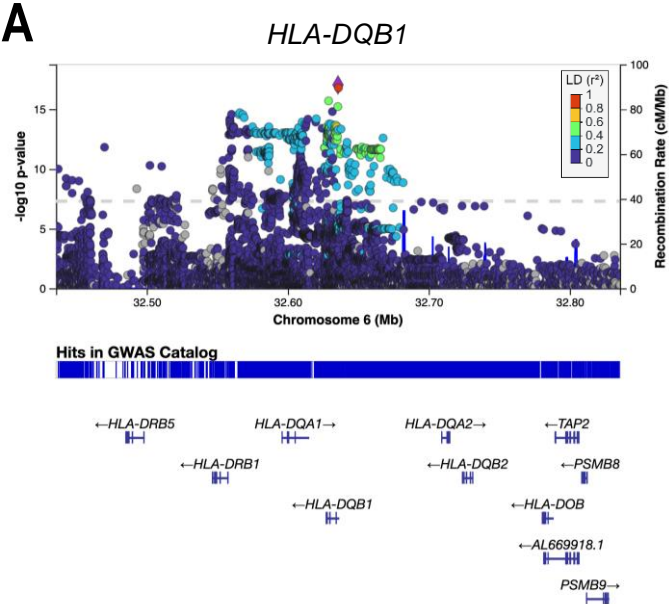


Fig. S5. Conditional analysis of *PLTP* and *MMP9* signals in the 20q13 locus. Regional association plots of: (A) the EA replication meta-analysis, demonstrating a primary signal near *PLTP*; (B) the IAMDGC study (8), demonstrating a primary signal near *MMP9*; (C) the EA meta-analysis conditioned on the index SNP from the IAMDGC study (rs1888235); (D) the IAMDGC study conditioned on the index SNP from the EA meta-analysis (rs17447545). LD r^2 values were calculated in the MVP EA cohort. The dashed line denotes genome-wide significance (5×10^{-8}).

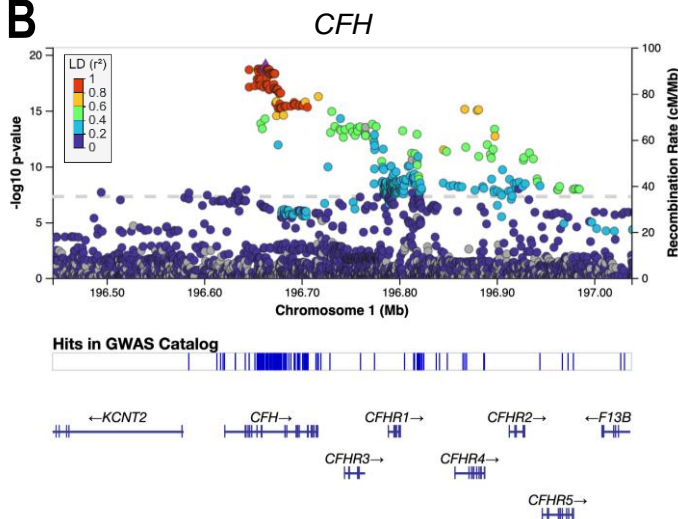
African-ancestry (AA) GWAS

A



Hispanic-ancestry (HA) GWAS

B



C

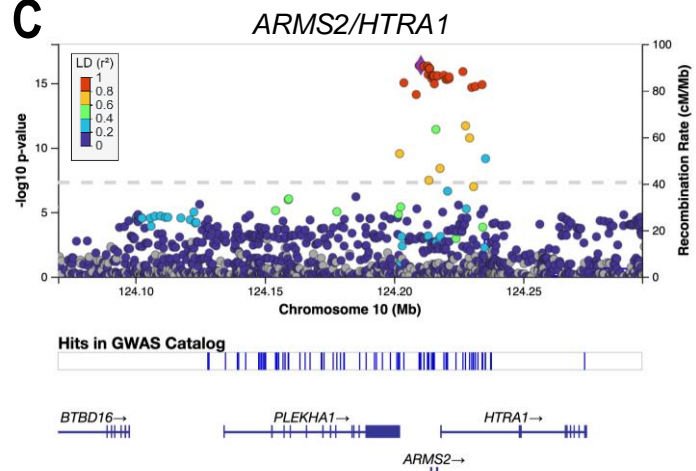


Fig. S6. Genome-wide significant loci from the AA and HA GWAS in MVP. (A) Regional association plot of the *HLA-DQB1* locus from the AA GWAS (2,302 cases, 29,223 controls). The 1000 Genomes AFR panel was used as the reference for plotting LD r^2 . (B-C) Regional association plots of the *CFH* and *ARMS2-HTRA1* loci from the HA GWAS (1,656 cases, 10,819 controls). The 1000 Genomes AMR panel was used as the reference for plotting LD r^2 .

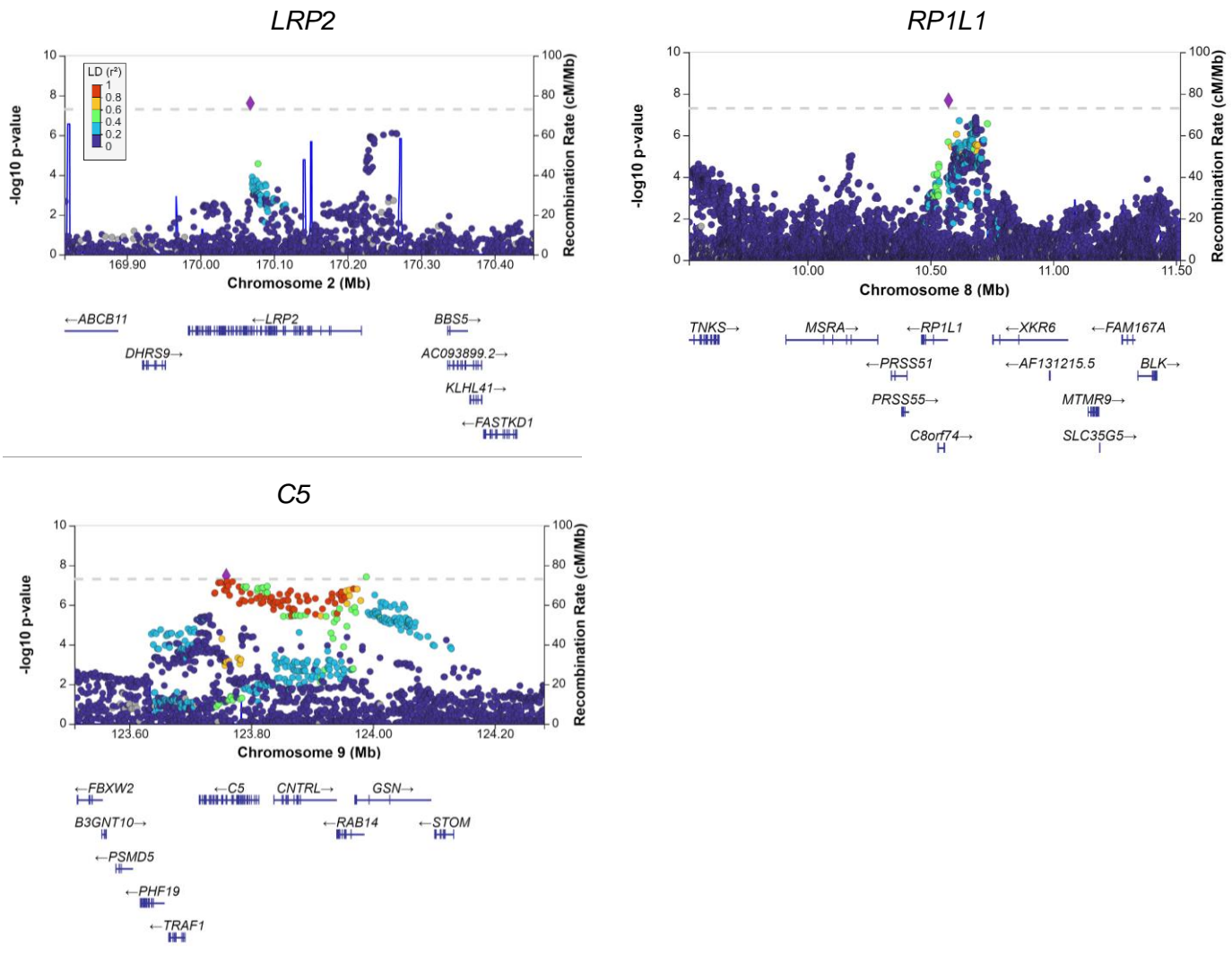
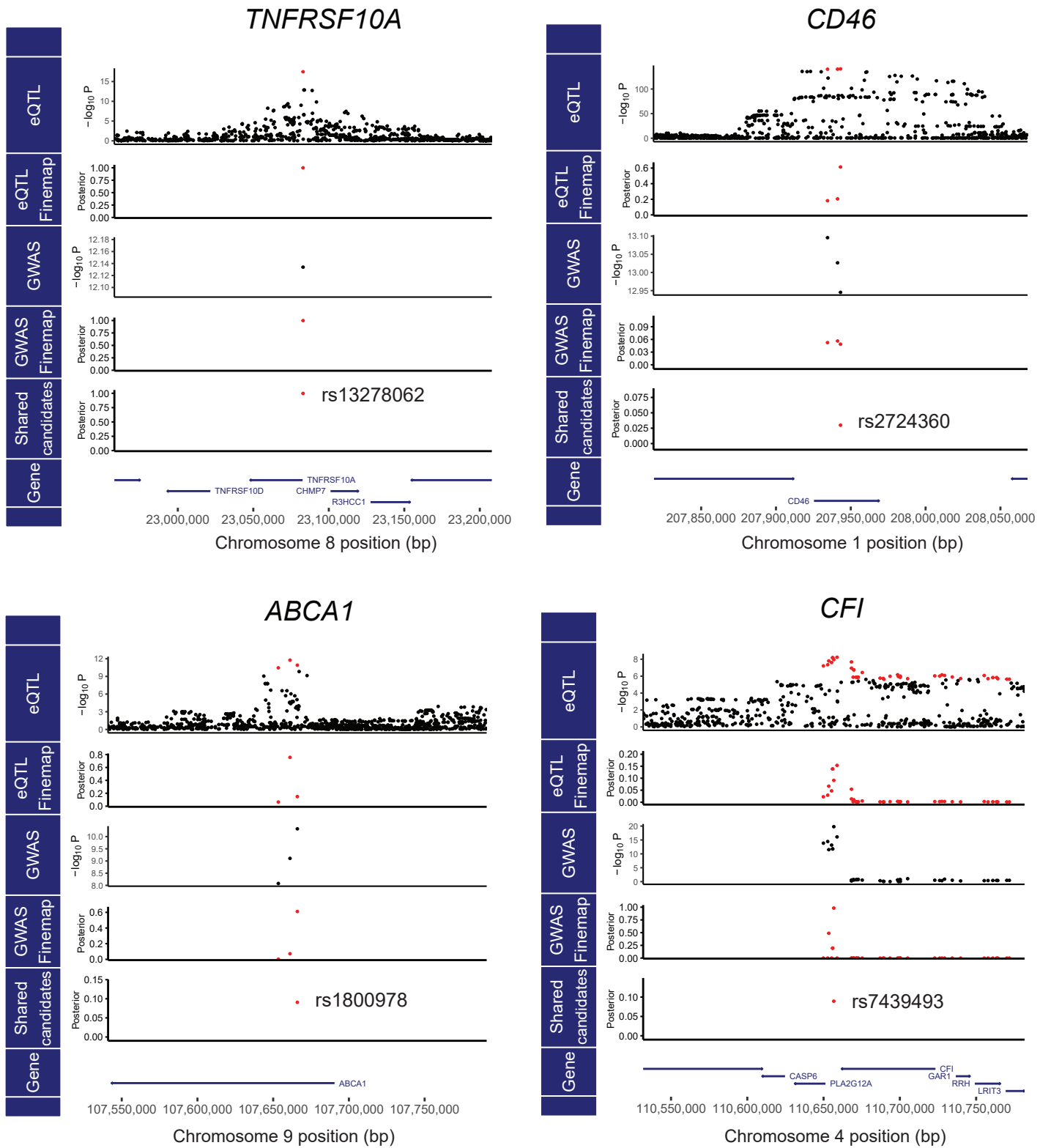
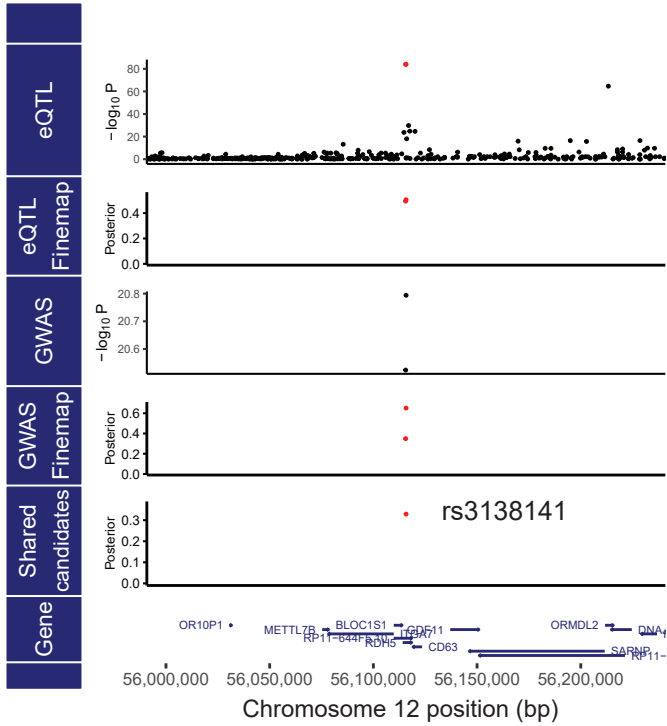


Fig. S7. Novel genome-wide significant loci from the multi-ancestry meta-analysis.
 Regional association plots of novel loci from the multi-ancestry replication meta-analysis (61,258 cases, 364,472 controls) beyond that reported for the EA meta-analysis. The 1000 Genomes EUR panel was used as the reference for plotting LD r^2 .

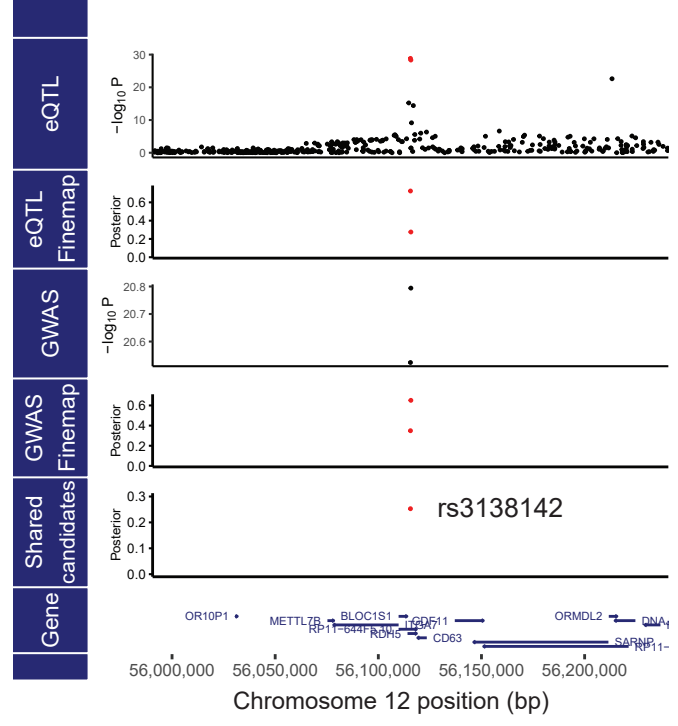
Fig. S8. Co-localization of GWAS and eQTL signals identifies candidate causal variants. Shown are significant co-localized signals (co-localization posterior probability > 0.01) from the multi-ancestry discovery meta-analysis using the mmQTL (31) method.



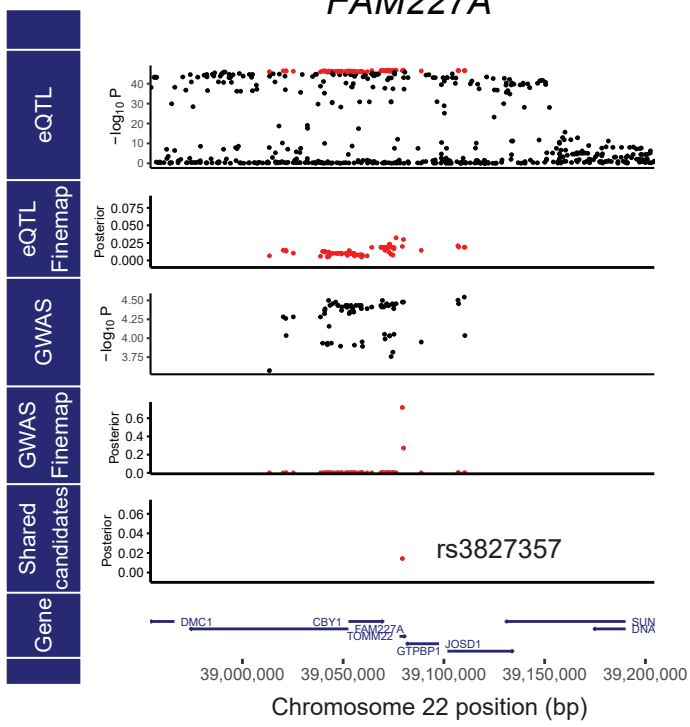
BLOC1S1



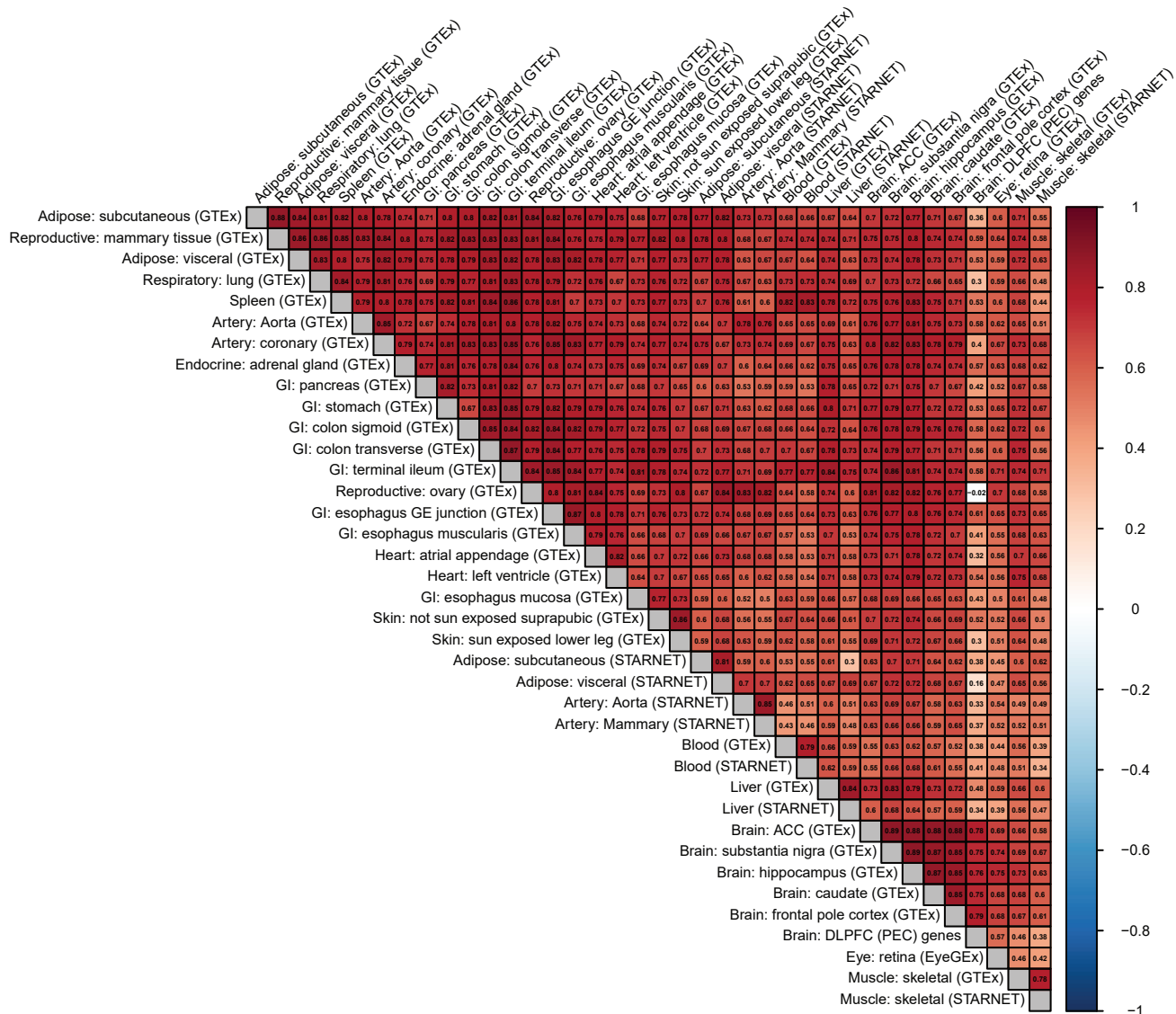
RDH5



FAM227A



A



B

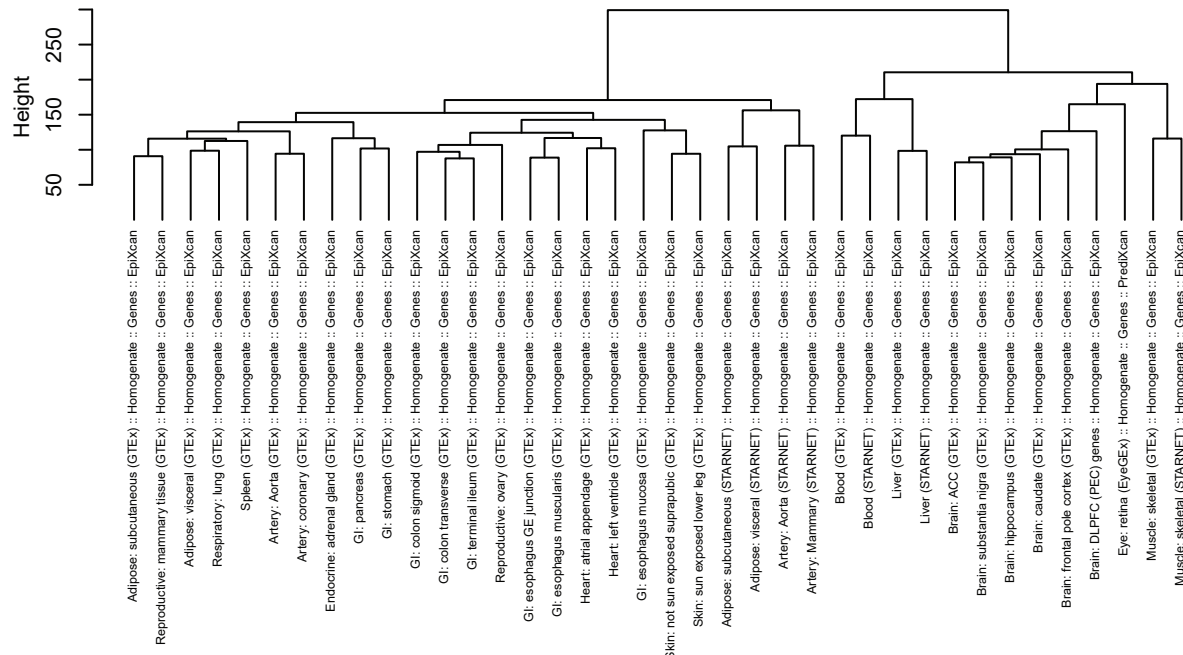
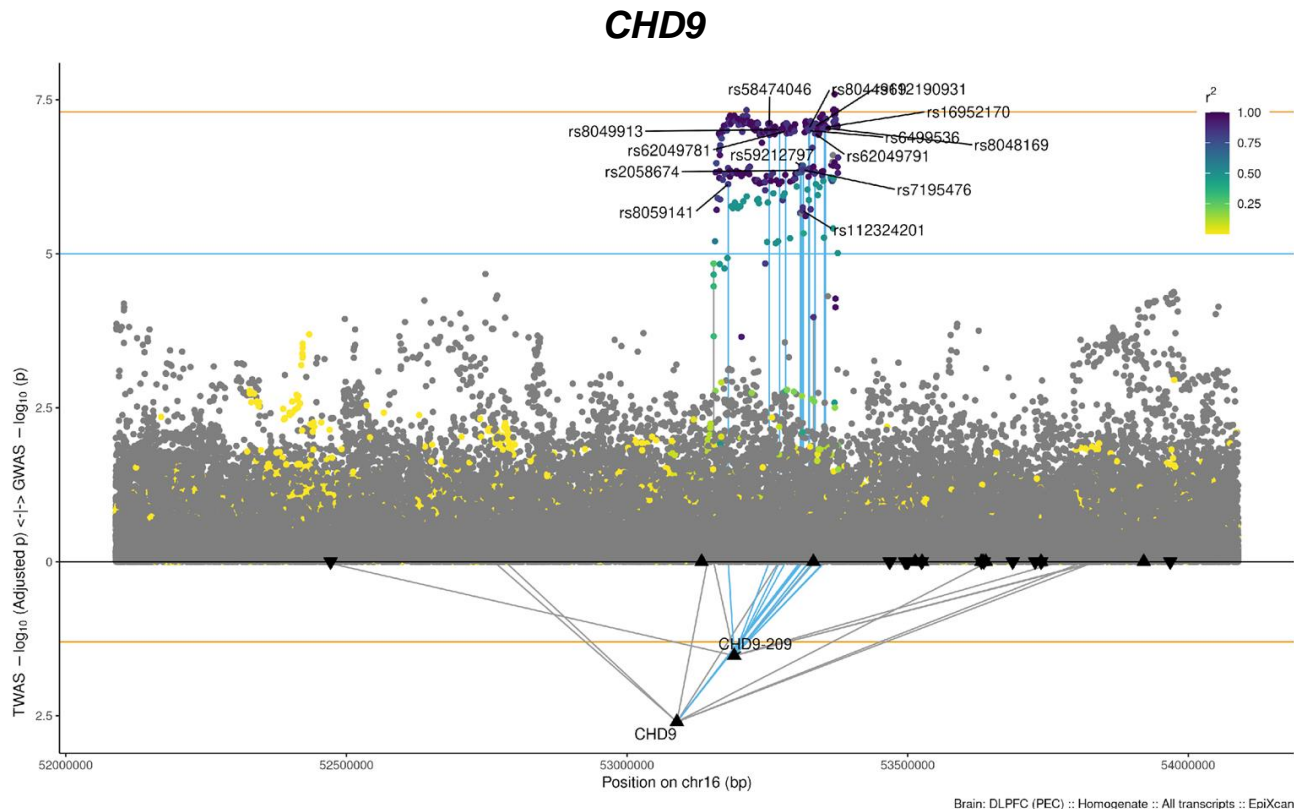
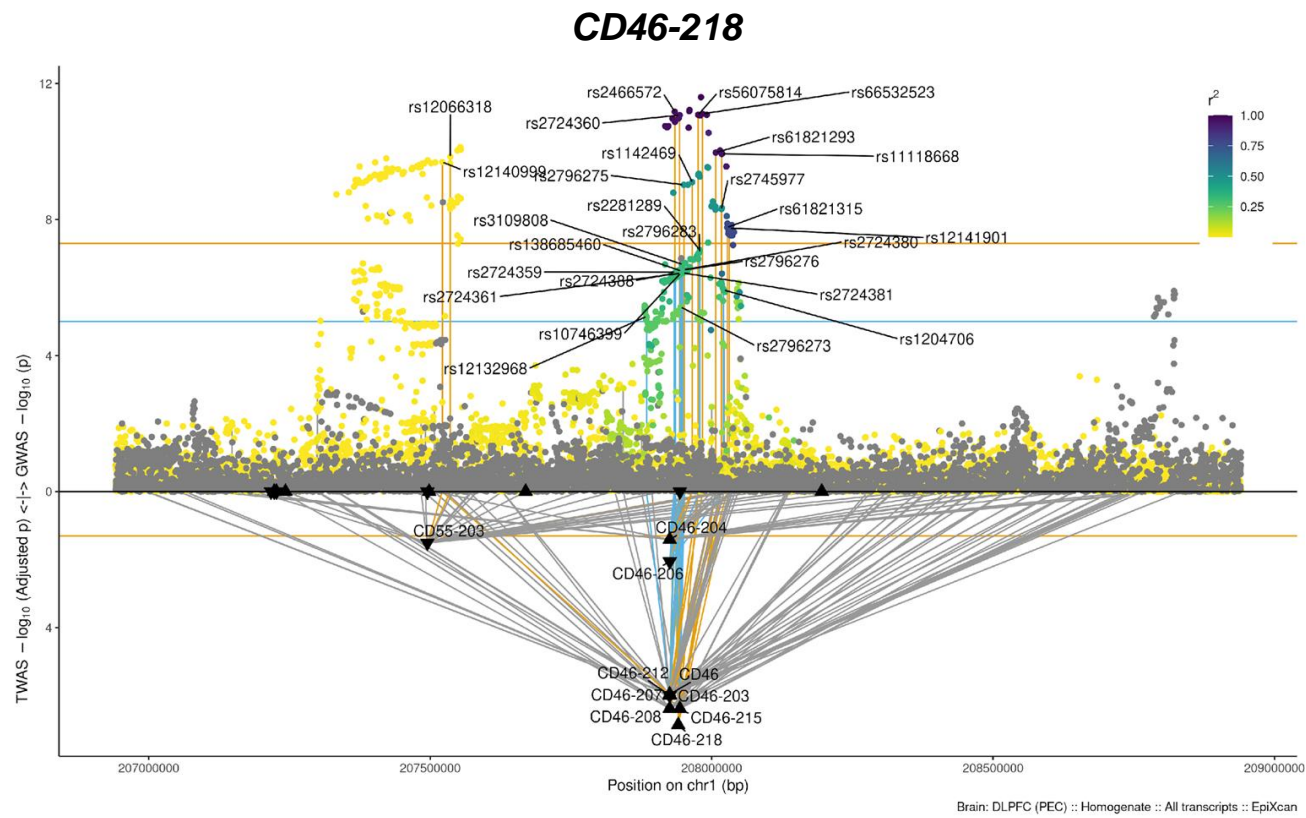
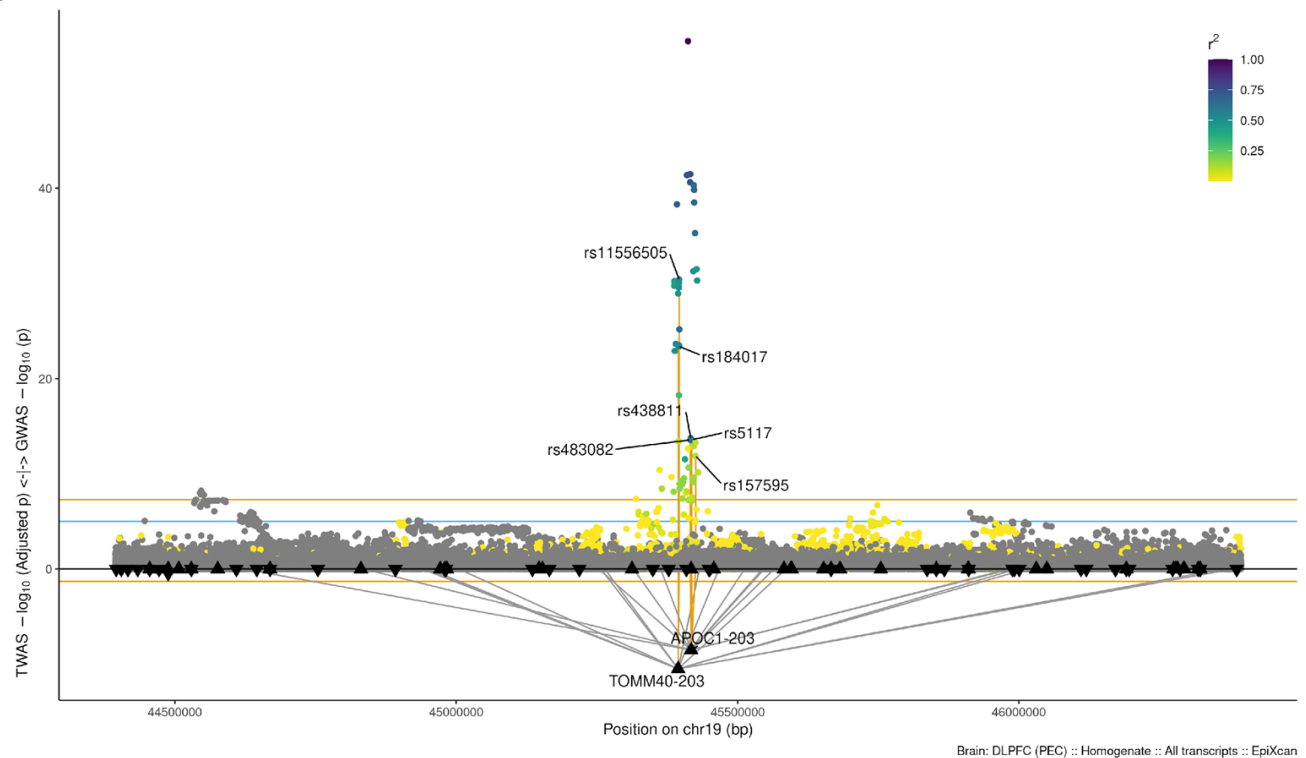


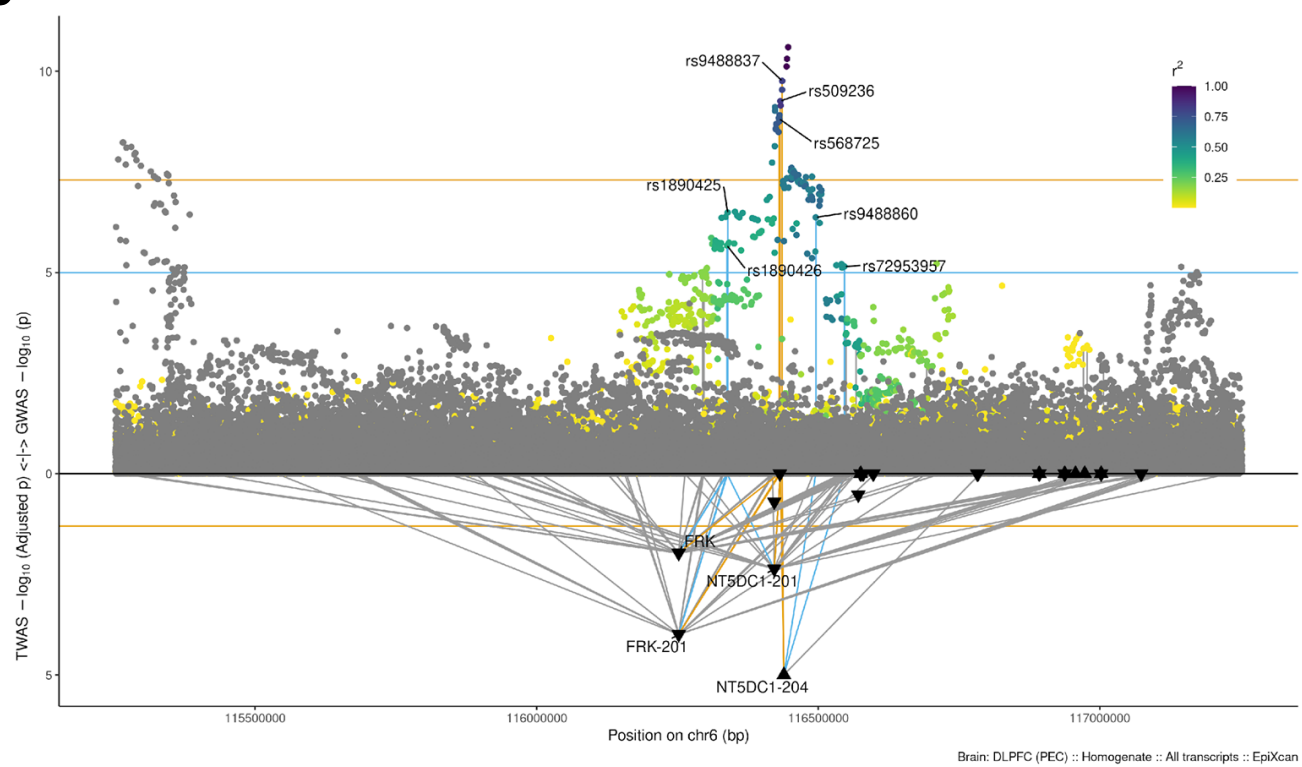
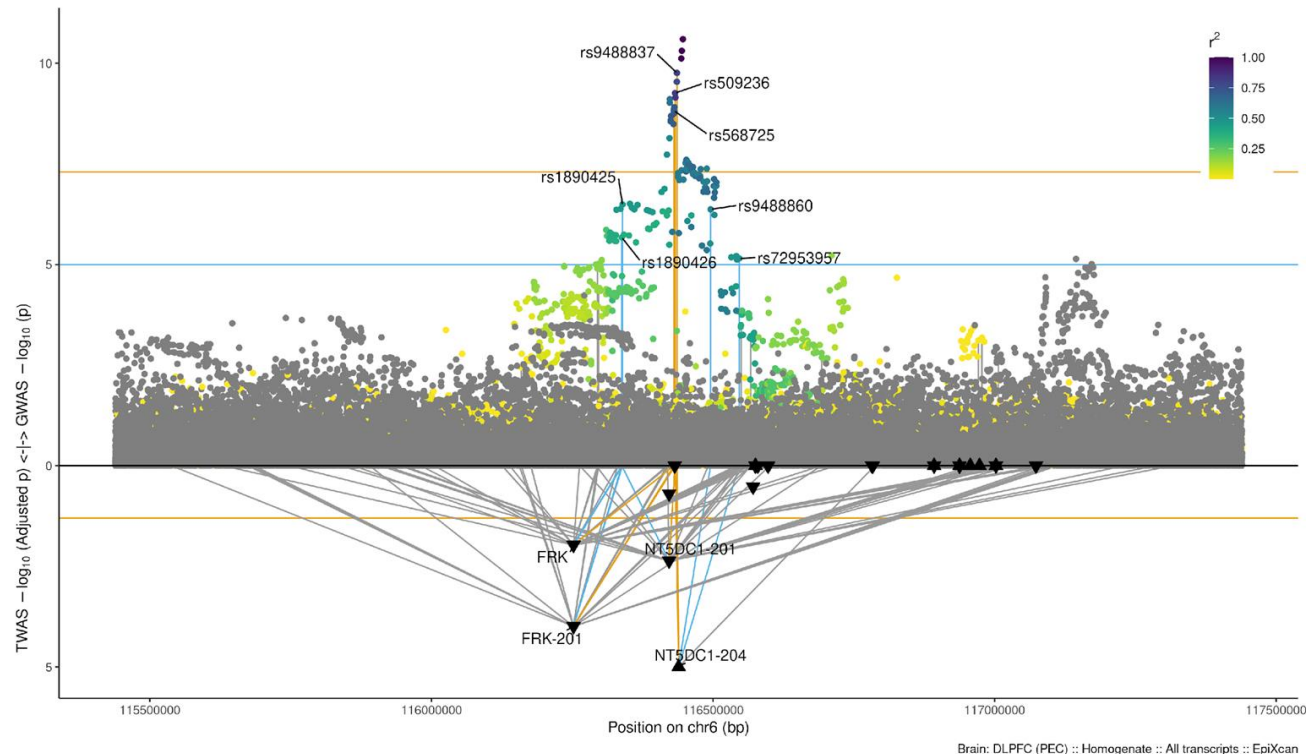
Fig. S9. Characterization of TWAS results across tissues. (A) Pearson correlation of AMD association z-scores across the 38 tissues analyzed from GTEx, EyeGEx, STARNET, and PEC. (B) Hierarchical clustering of tissues based on AMD associations using Ward's linkage method.

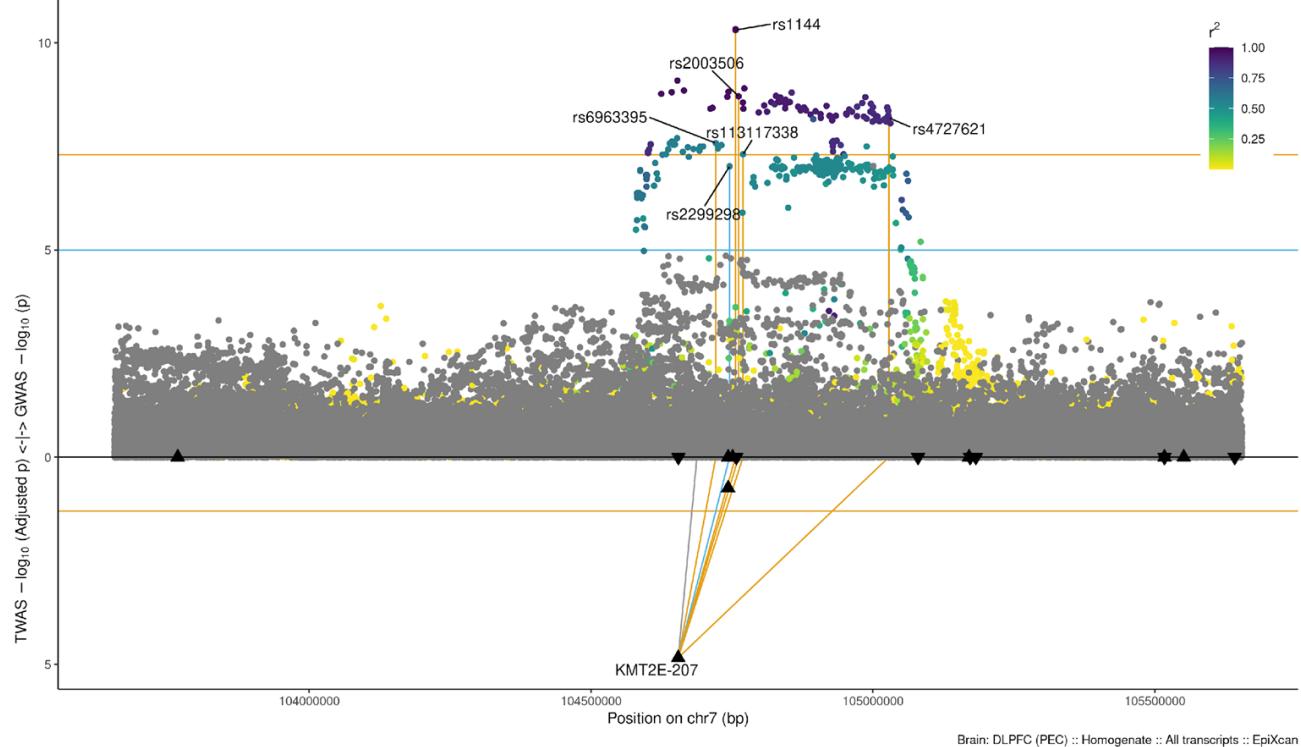
Fig. S10. Regional Miami plots of genes with novel TWAS associations. The TWAS was based on the DLPFC brain model jointly testing genes and transcript isoforms. Results are based on the EA discovery meta-analysis (N=45,045 cases, 275,806 controls). The GWAS p-values are shown above the $y=0$ line, and the TWAS p-values are shown below it. SNPs are colored according to linkage disequilibrium r-squared with the lead SNP (EA panel). Lines connecting SNP predictors of genetically regulated gene expression are colored according to the significance level of the SNP: orange, $p \leq 5 \times 10^{-8}$; cyan, $p \leq 1 \times 10^{-5}$; gray, $p > 1 \times 10^{-5}$.

A

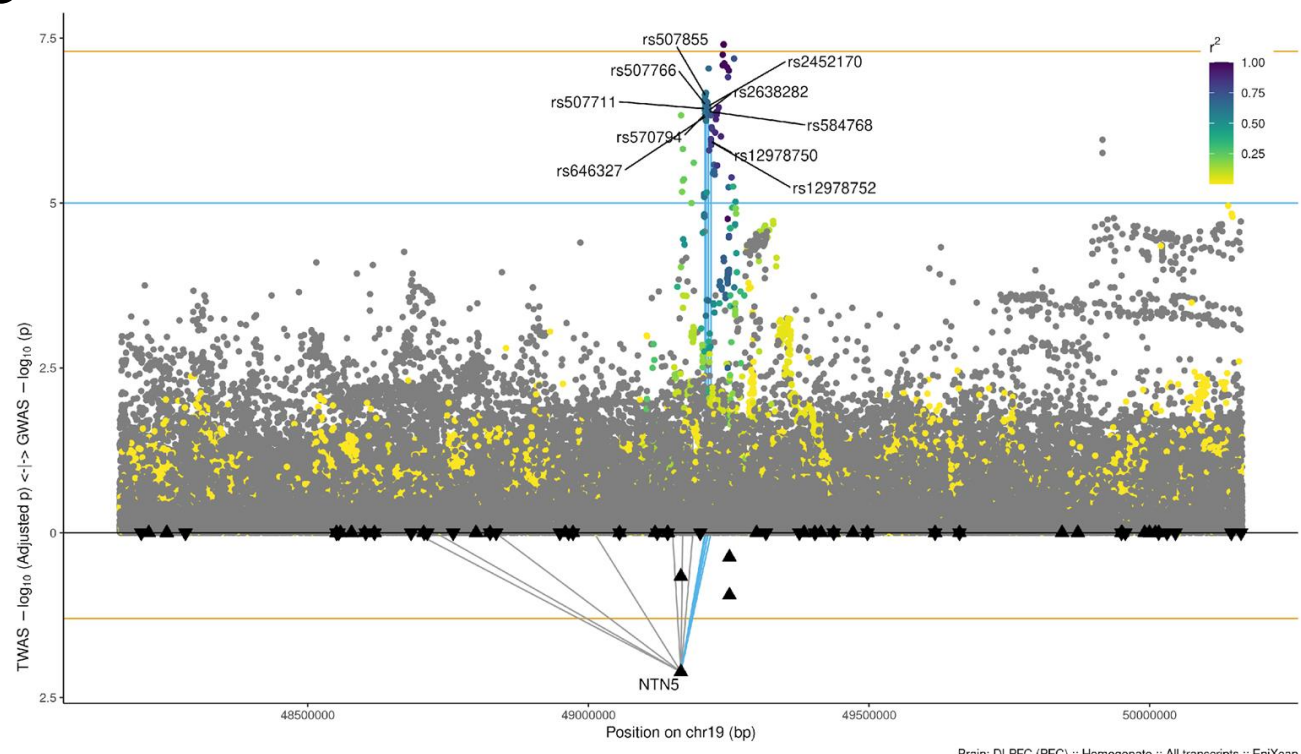


B**C**

D***FRK-201*****E*****NT5DC1-204***

F**KMT2E-207**

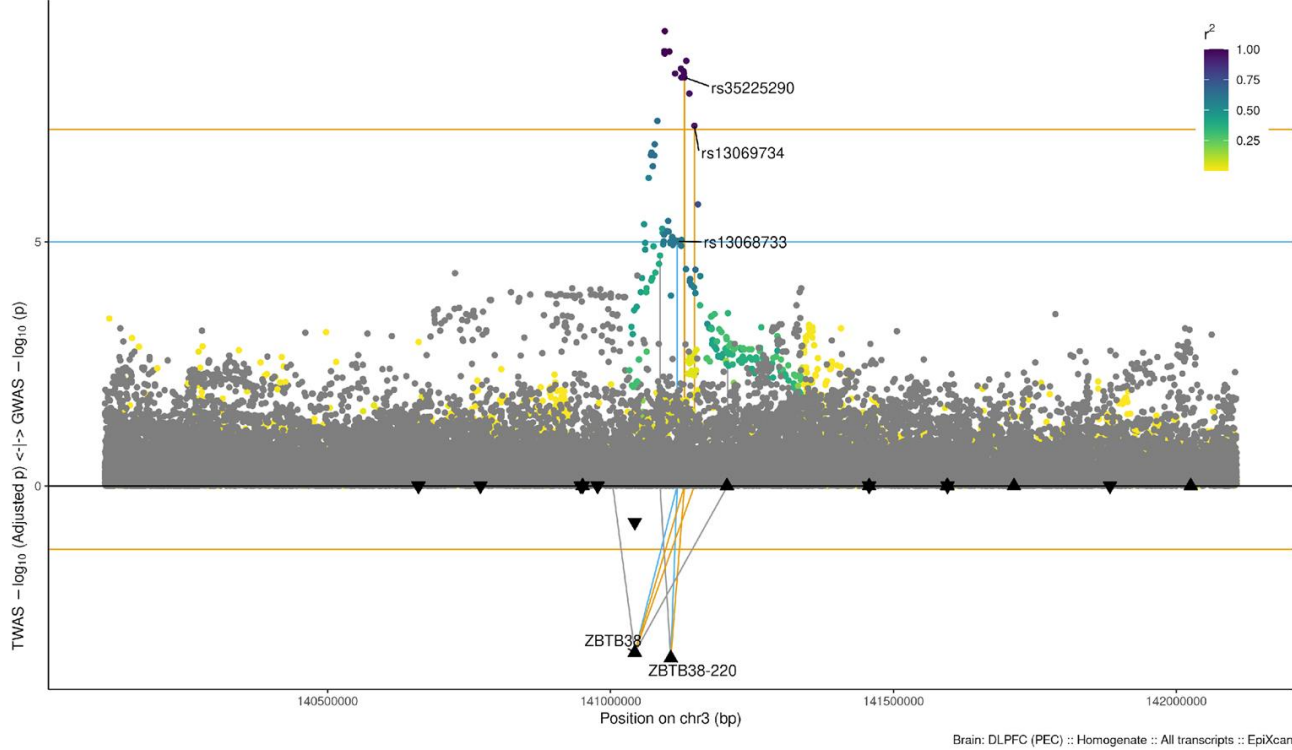
Brain: DLPFC (PEC) :: Homogenate :: All transcripts :: EpiXcan

G**NTN5**

Brain: DLPFC (PEC) :: Homogenate :: All transcripts :: EpiXcan

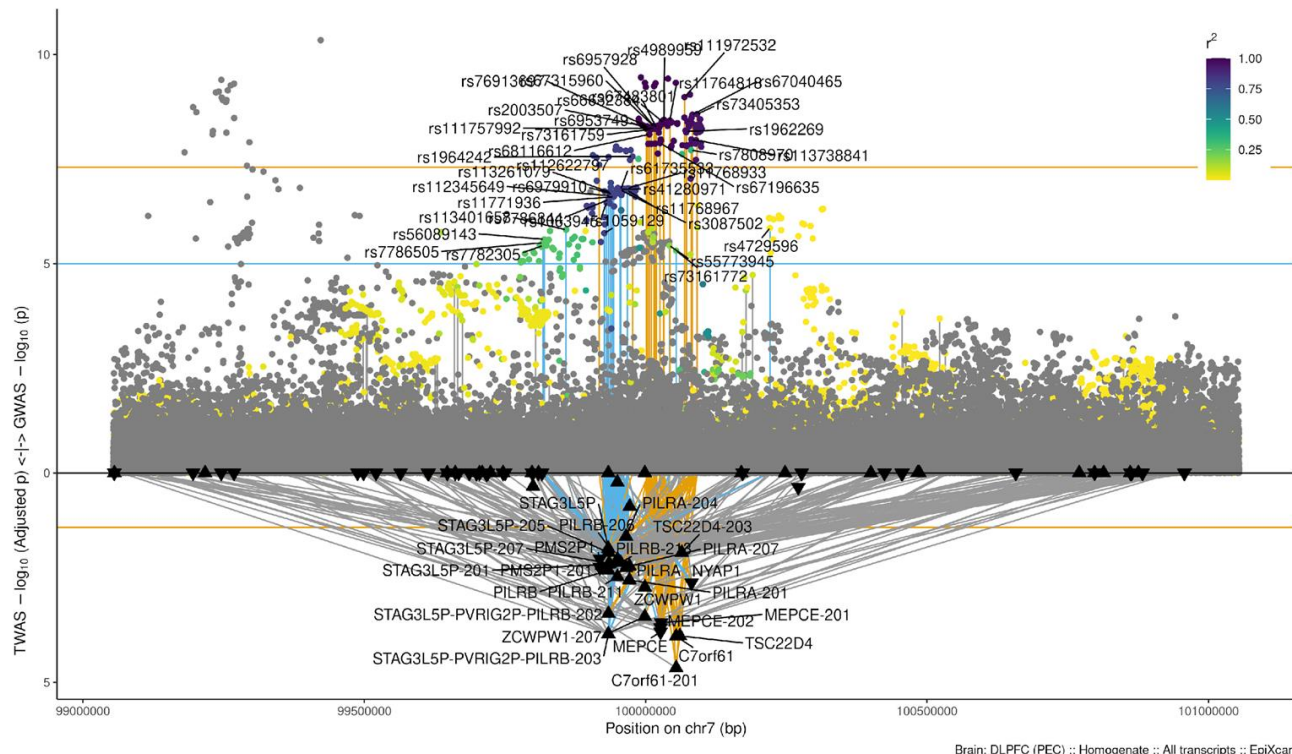
H

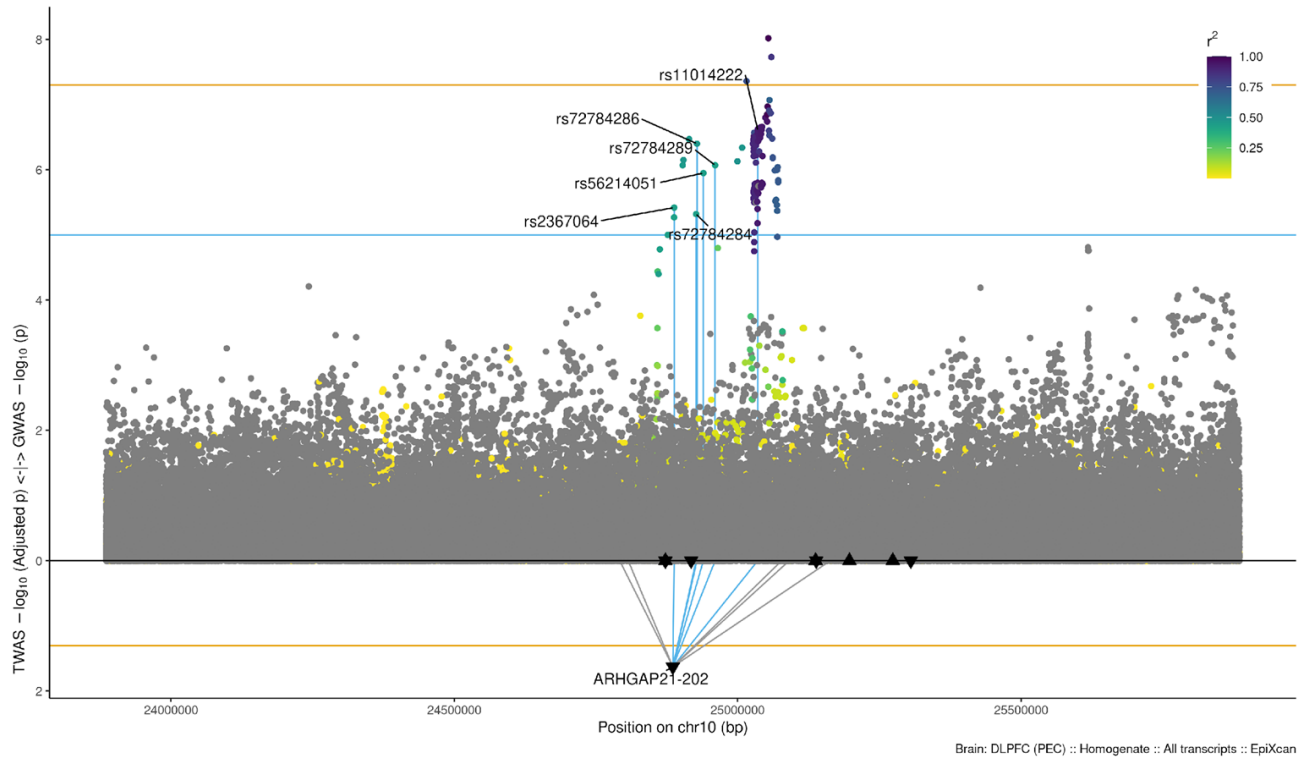
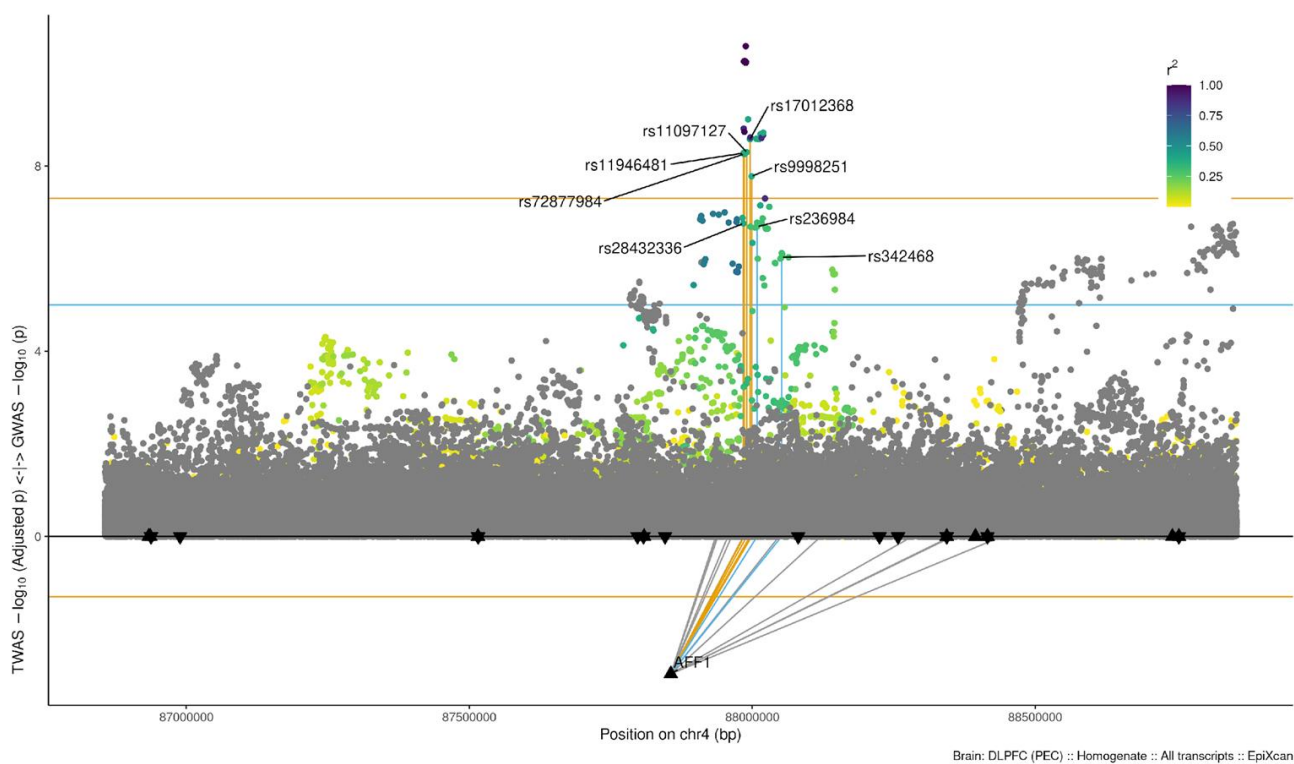
ZBTB38-220

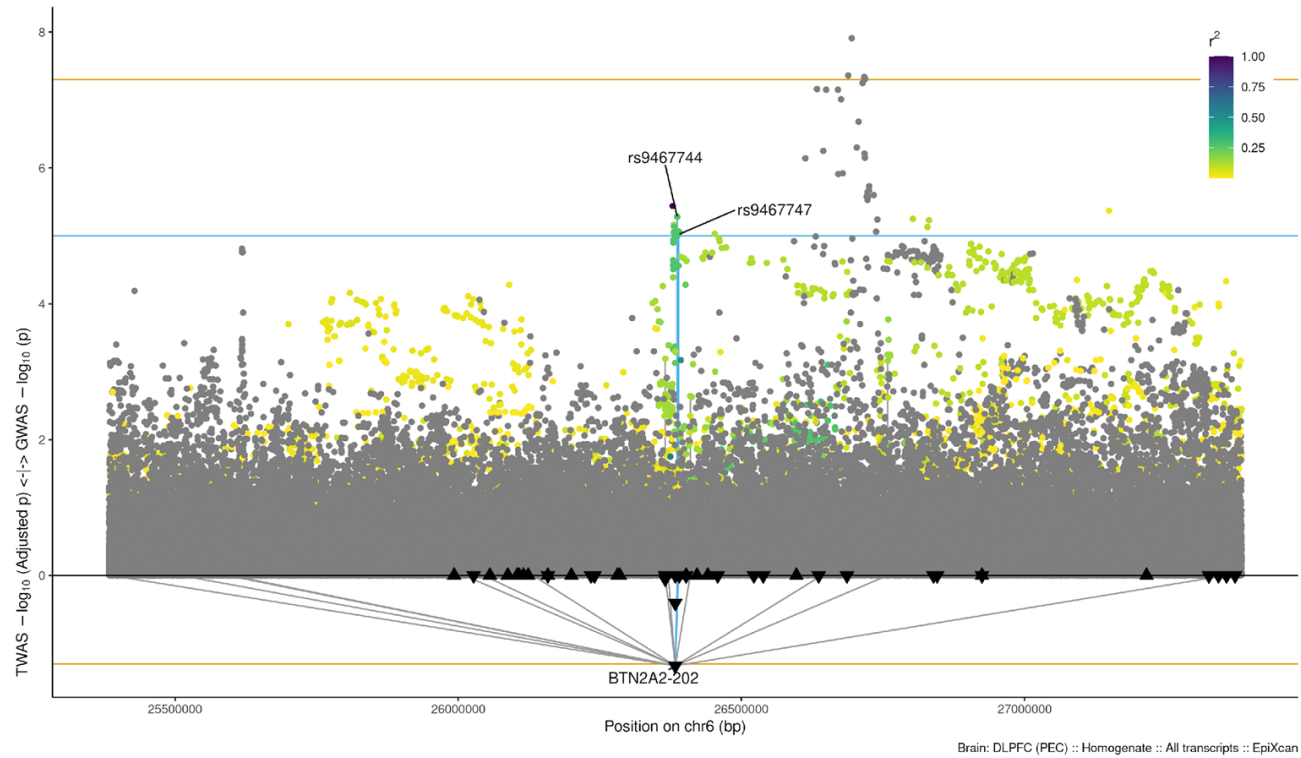
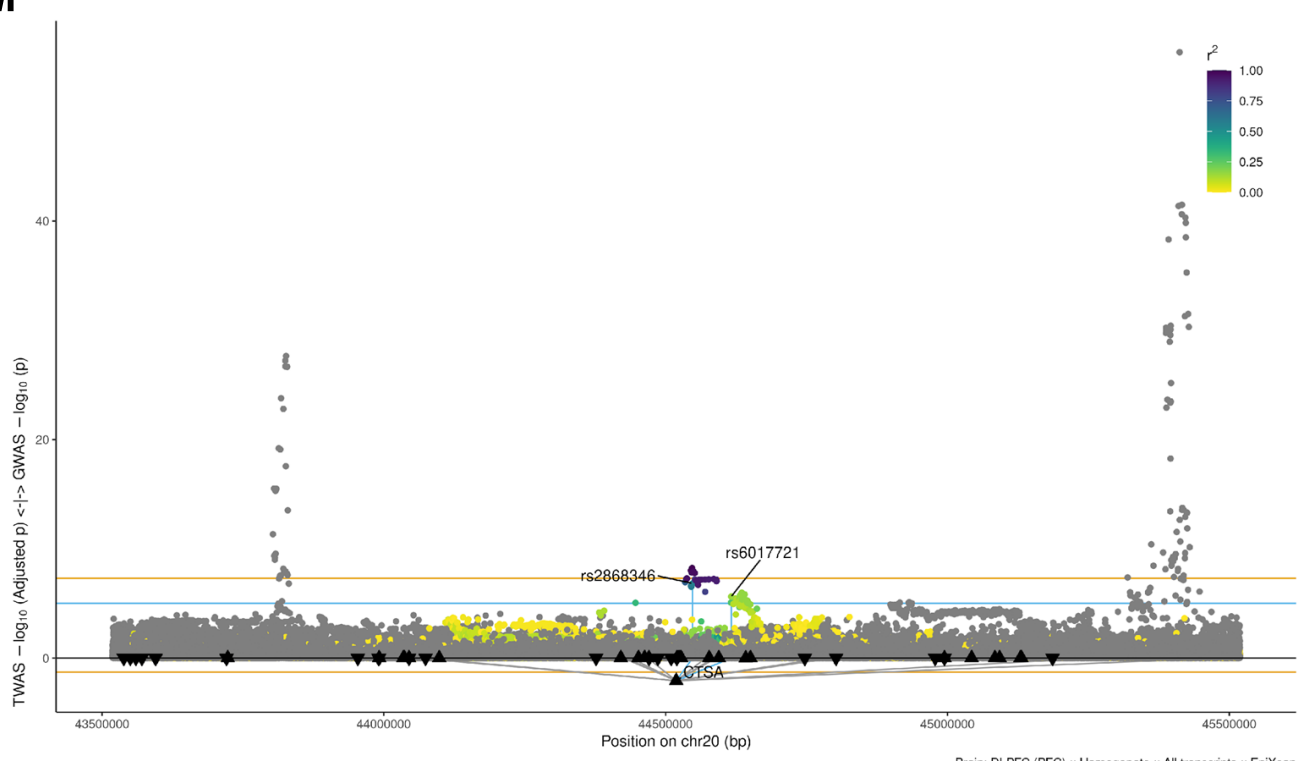


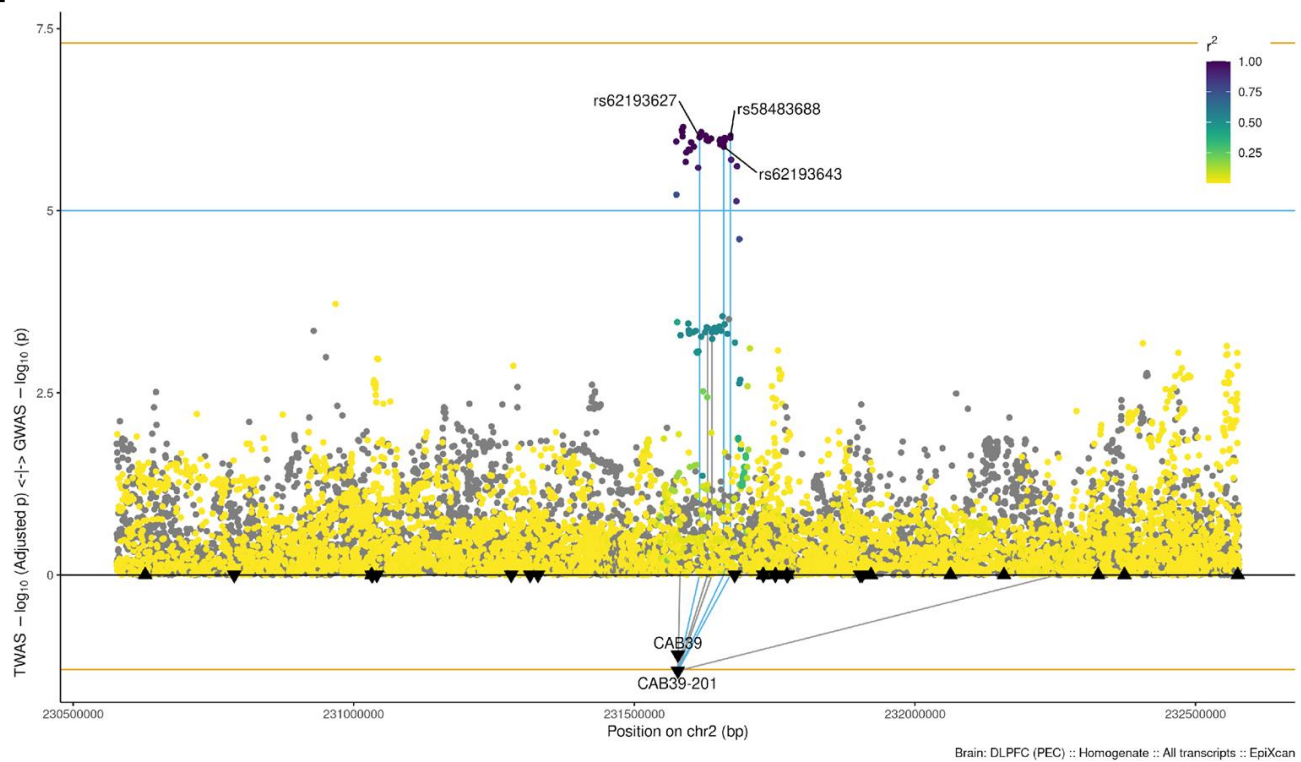
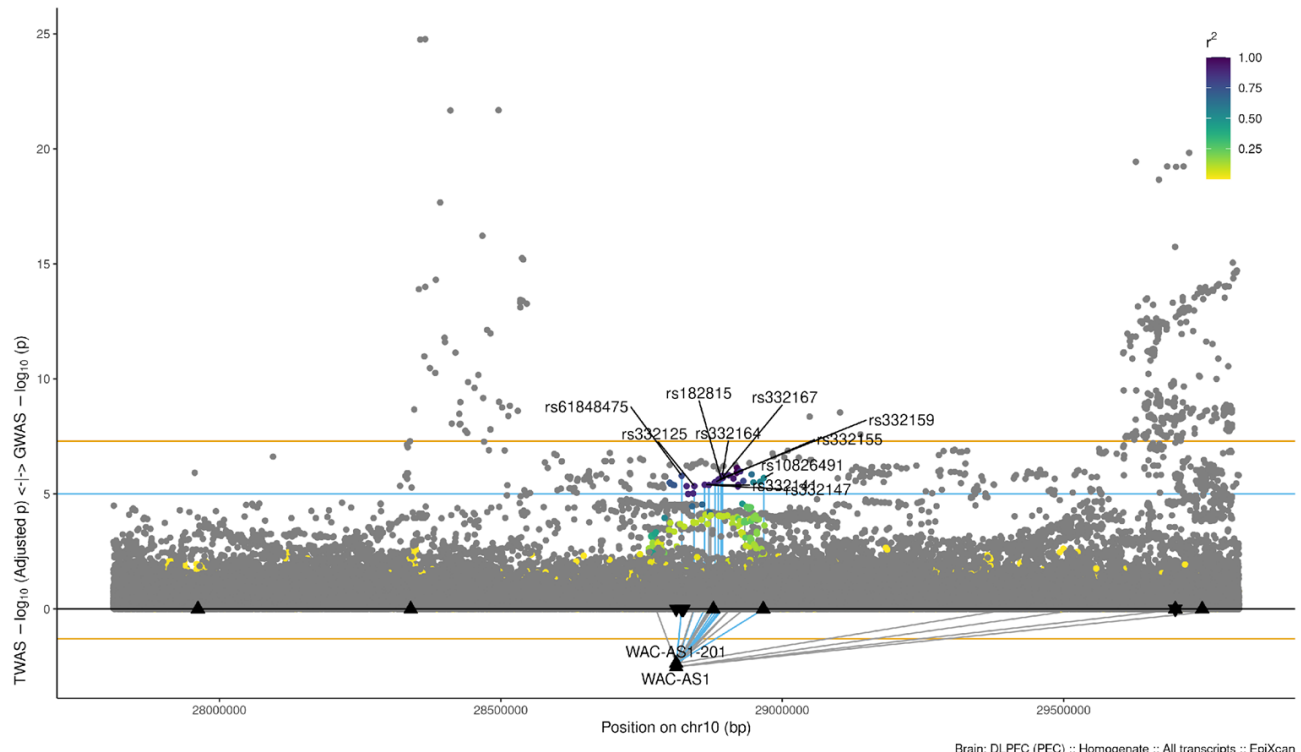
1

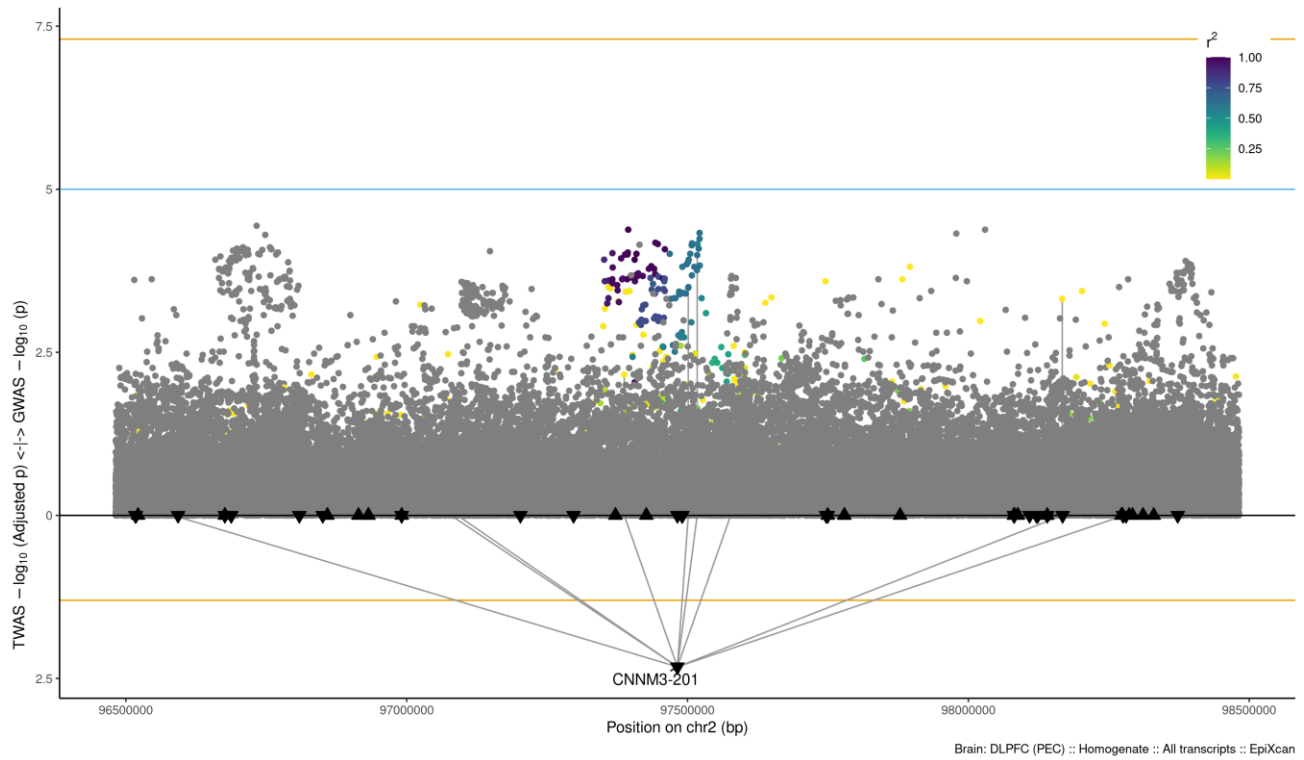
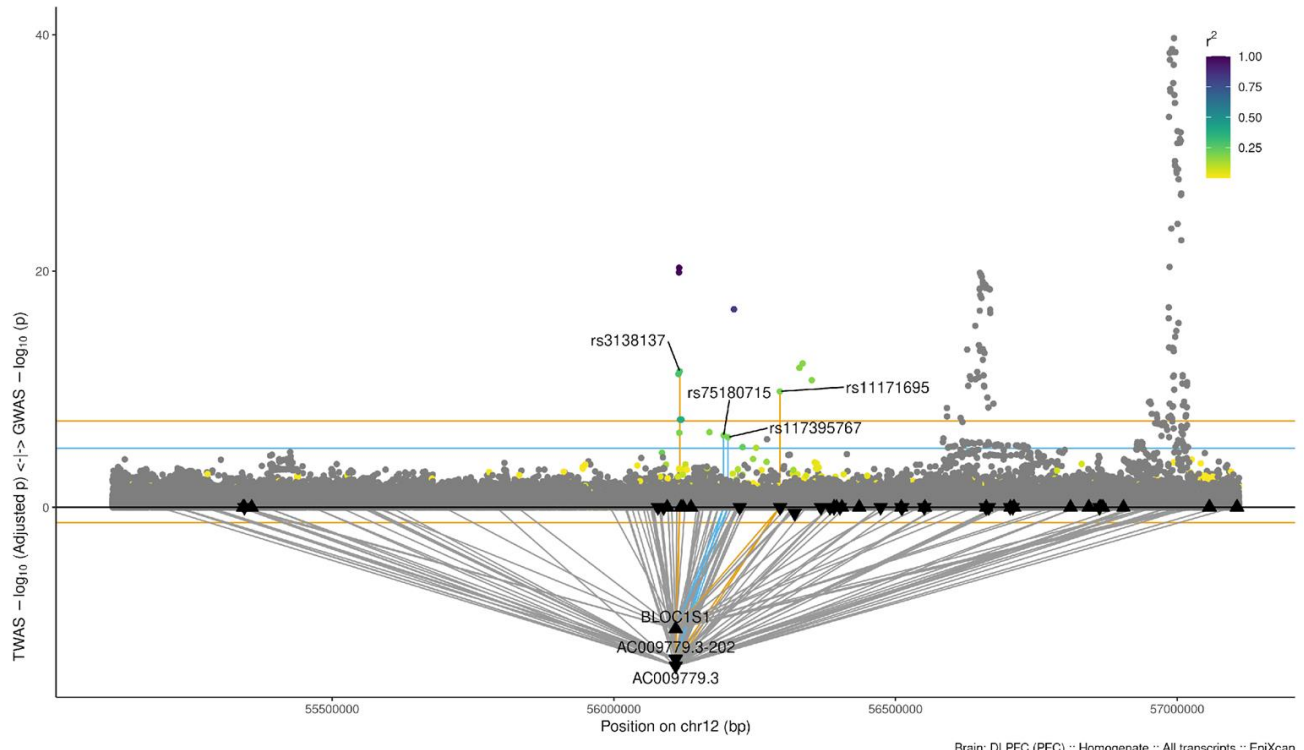
C7orf61-201

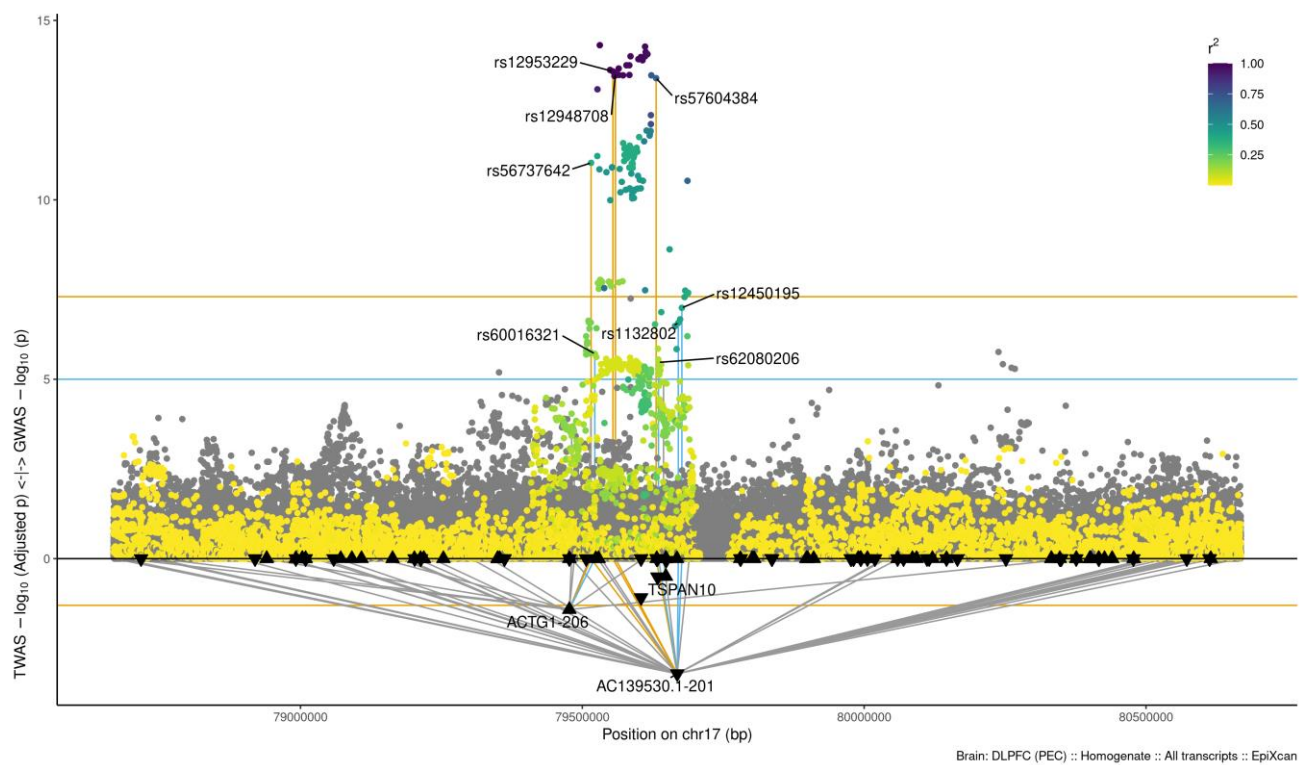
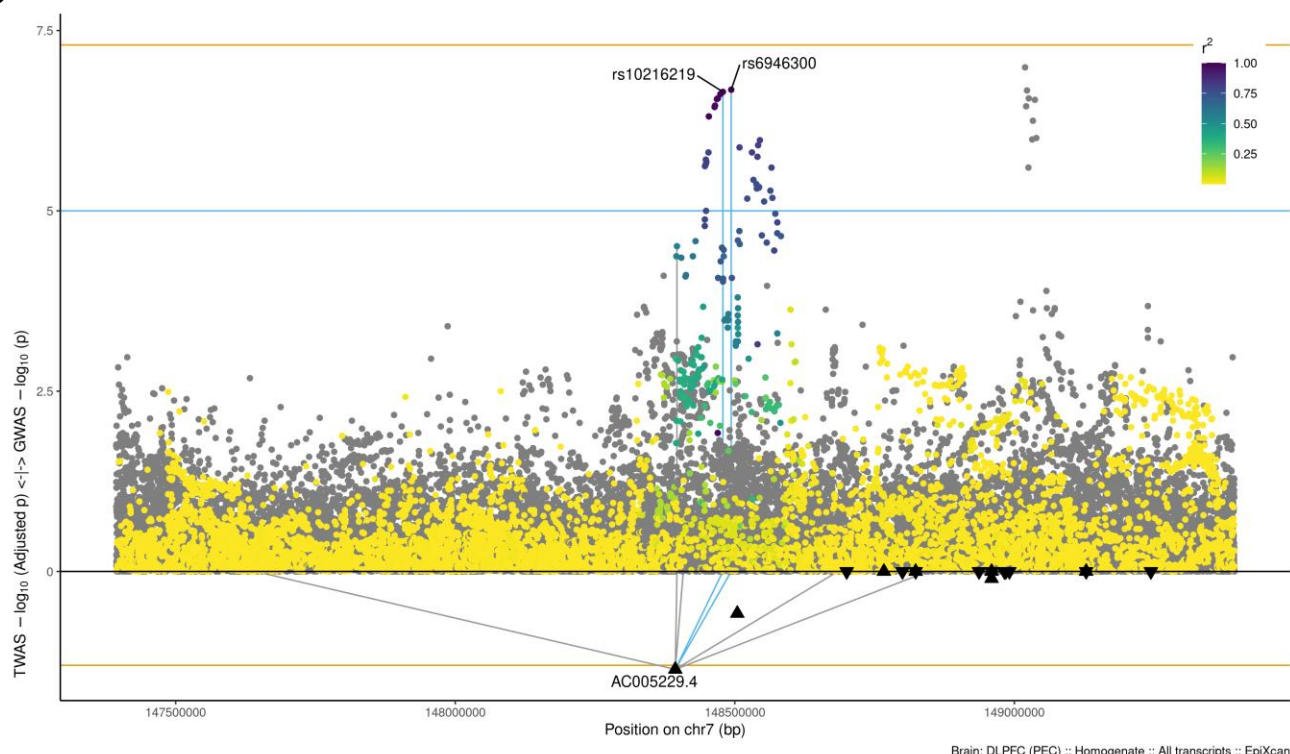


J***ARHGAP21-202*****K*****AFF1***

L**BTN2A2-202****CTSA**

N**CAB39-201****O****WAC-AS1**

P**CNNM3-201****Q****AC009779.3**

R**AC139530.1-201****S****AC005229.4**

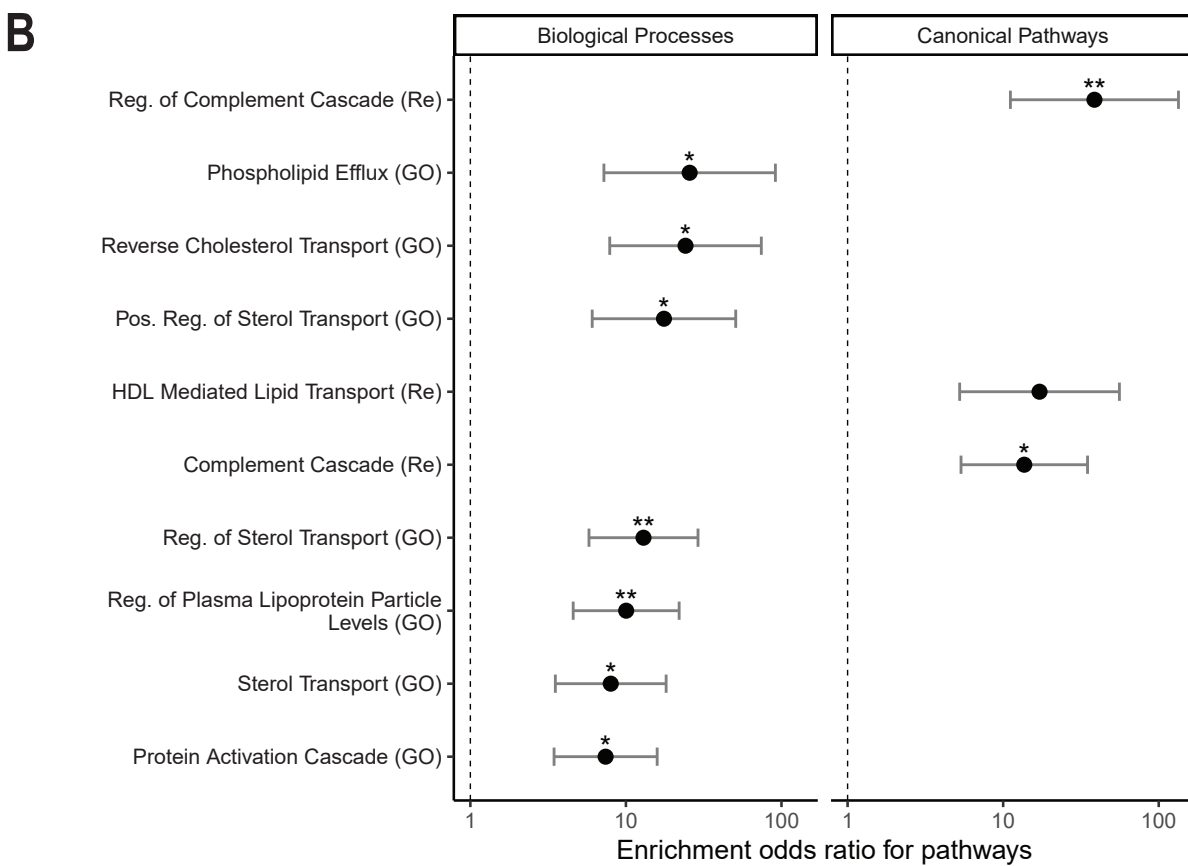
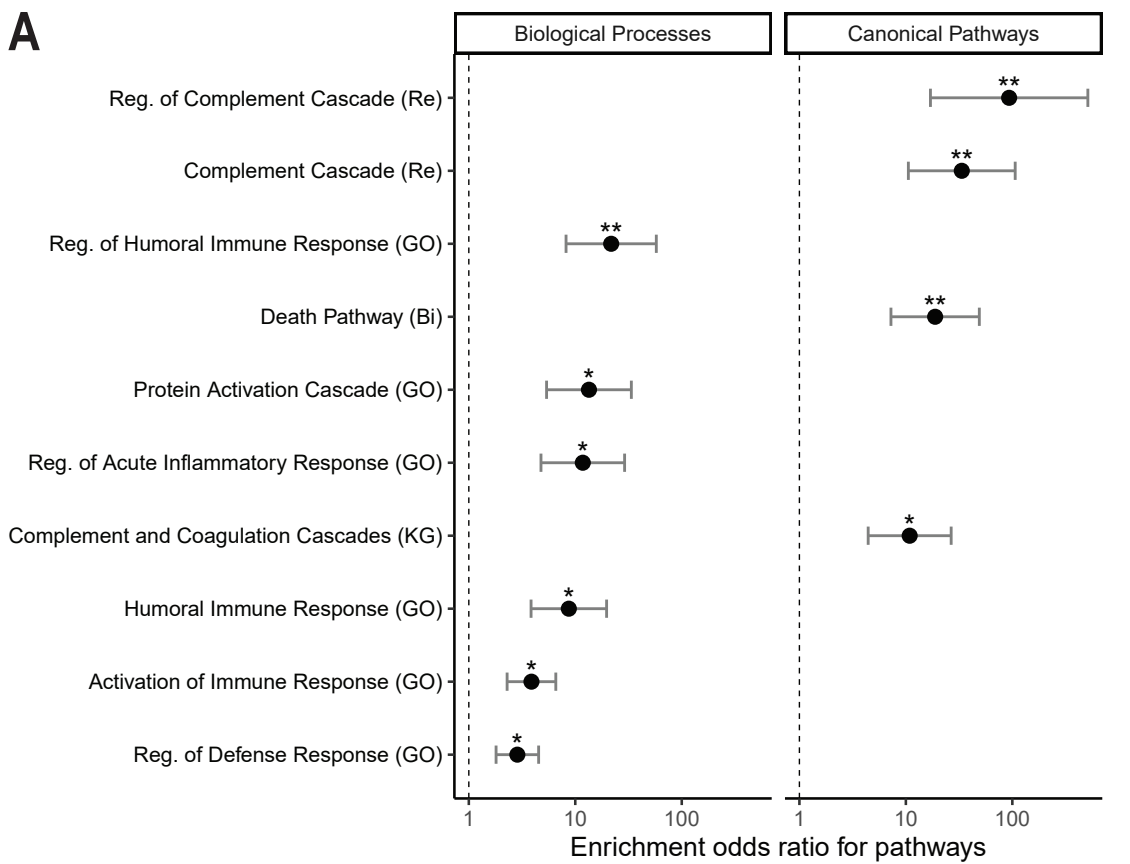


Fig. S11. Gene set enrichment analysis (GSEA) of TWAS genes. (A) GSEA of TWAS using the DLPFC transcripts (genes and isoforms) model, and **(B)** the multi-tissue meta-analysis. Shown are the top ten enrichments by effect size (odds ratio) in both analyses.



Fig. S12. Semantic clustering of enriched gene ontology (GO) terms in the AMD multi-tissue transcriptome-wide association study (TWAS) identifies immune and lipid homeostasis functions. First, we performed enrichment of AMD TWAS associated genes ($FDR < 0.05$ in ACAT meta-analysis of all tissues) for GO terms corresponding to ontologies of molecular functions (MFO), biological processes (BPO), and cellular components (CCO). Semantic clustering of the GO terms that had enrichment $FDR < 0.1$ (Fisher's exact test) and could be clustered identified 7 clusters (BPO1-BPO5, CCO1, and MFO1). For each of these clusters we provide a word cloud based on the description of the GO terms where words that appear more frequently are larger; clusters are ordered from left to right and top to bottom from the most significant to the least significant based on their meta-analyzed p-value (ACAT). Major themes that are associated with AMD are immune functions and lipid homeostasis.

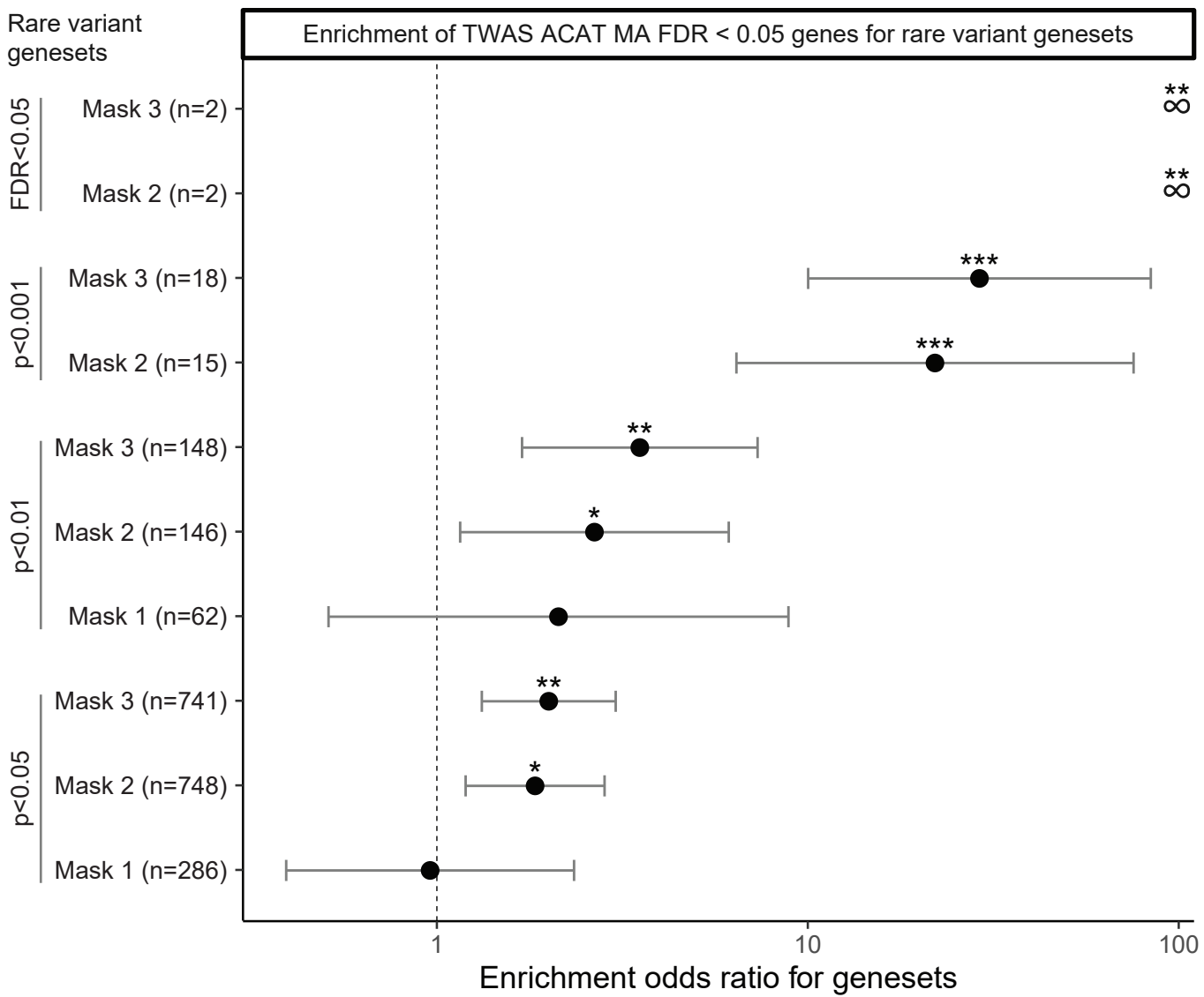


Fig. S13. Enrichment of rare variant burden associations in TWAS meta-analysis genes. TWAS meta-analysis genes were those with FDR < 0.05; only protein-coding genes were considered. *** FDR < 0.001, ** FDR < 0.01, * FDR < 0.05 (12 rare variant gene sets were considered from the rare variant analysis). Mask 1: Loss of function mutations only; Mask 2: Loss of function + missense mutations; Mask 3: Loss of function + missense + splice mutations.